[Short title + Author Name - P&H title] 17 (2024) 105987

Contents lists available at ScienceDirect

Arabian Journal of Chemistry

journal homepage: www.ksu.edu.sa

Design and synthesis of ladder-type covalent organic frameworks

Hongfei Sun [a,*], Xianying Wu [a], Bin Yao [a], Guowang Li [a], Ning Qi [a], Lei Shi [b,*]

[a] Chongqing Key Laboratory of Catalysis and Functional Organic Molecules, College of Environment and Resources, Chongqing Technology and Business University, Chongqing 400067, China
[b] State Key Laboratory of Fine Chemicals, Dalian University of Technology, Dalian 116024, China

ARTICLE INFO

Keywords:
Ladder-type
Covalent organic frameworks
Topology design
Condensation reaction
Nucleophilic aromatic substitution reaction

ABSTRACT

Covalent organic frameworks (COFs) are typical porous organic polymers with crystalline porous architectures, which are provided with the merits of high surface area, low density, and high structural as well as functional adjustability. In comparison to conventional COFs with single-stranded linkages, ladder-type COFs are a very unique class of COFs which are usually connected by rings (conjugated or non-conjugated). Given the structural characteristics of ladder-type COFs, they overcome the shortcomings of conventional COFs and possess the advantages of rigid backbone, extended π-conjugation length, extraordinary chemical/thermal stability, and high conductivity. However, compared to the well-investigated conventional COFs, ladder-type COFs are paid little attention. Gaining ladder-type COFs quickly and efficiently encounters great challenges. Ladder-type COFs, containing a wide array of structures and functionalities, have recently come into focus. Especially for energy conversion and storage, they show great potential with excellent performances. Accordingly, this article systematically summarizes the recent developments in constructing ladder-type COFs. Initially, the topology design is generally introduced. Subsequently, the synthesis of ladder-type COFs is discussed in detail. It shows how to rationally select organic reactions and monomers and how to manipulate experimental conditions to construct ladder-type COFs bearing different functional groups and different conjugation lengths. Ultimately, this paper offers a concise outlook on the prospective advancements in the synthesis of ladder-type COFs.

1. Introduction

Porous organic polymers (POPs) are a very important class of porous materials, the building units of which are covalently linked by light elements including boron, carbon, nitrogen, oxygen, and silicon (Das et al., 2017; Zhu et al., 2020; Evans et al., 2022; Qi et al., 2023). They are endowed with diverse advantages such as low density, high stability and high Brunauer–Emmett–Teller (BET) surface area, and thus have been widely used in environment, energy, and catalysis fields. There are many kinds of POPs such as hyper cross-linked polymers (HCPs) (Xu et al., 2013), polymers of intrinsic microporosity (PIMs) (McKeown 2017), conjugated microporous polymers (CMPs) (Lee and Cooper, 2020; Luo et al., 2021), porous aromatic frameworks (PAFs) (Pei et al., 2015; Tian and Zhu, 2020), fused aromatic networks (FANs) (Mahmood et al., 2019; Ahmad et al., 2020), and covalent organic frameworks (COFs) (Waller et al., 2015; Geng et al., 2020a; Geng et al., 2020b). Undoubtedly, provided with periodic crystalline structures, COFs are very bright stars among them. Owing to their well-defined pore shapes and sizes, ultrahigh BET surface areas, abundant and tunable structural units, COFs have gained greatly developed in various fields since it was firstly reported by Omar M. Yaghi in 2005 (Côté et al., 2005), such as synthetic strategies (*e.g.*, three dimensional COFs, heteroporous COFs, and post-synthetic functionalization) (Liang et al., 2020; Yusran et al., 2020; Guan et al., 2022; Phan et al., 2023), properties investigations (*e.g.*, chirality, crystallinity and stability, luminescent and photophysical properties) (Han et al., 2020; Haug et al., 2020; Huang et al., 2020b),

Abbreviations: BBL, Benzimidazobenophenanthroline; BET, Brunauer–Emmett–Teller; BHCC, Buchwald–Hartwig cross-coupling; CMPs, Conjugated microporous polymers; COFs, Covalent organic frameworks; DBU, 1,8-Diazabicyclo(5,4,0)undec-7-ene; DDQ, 2,3-Dichloro-5,6-dicyano-p-benzoquinone; DLS, Dynamic light scattering; FANs, Fused aromatic networks; EPR, Electron paramagnetic resonance; HAT, 1,4,5,8,9,12-Hexaazatriphenylene; HAT-CN, Hexaazatriphenylene-hexacarbonitrile; HATN, Hexaazatrinaphthalene; HBTP, 2,3,6,7,10,11-hexabromotriphenylene; HCPs, Hyper cross-linked polymers; PEEK, Polyetheretherketone; PMDA, Pyromellitic dianhydride; PIMs, Polymers of intrinsic microporosity; POPs, Porous organic polymers; PSF, polysulfone; S_NAr, Nucleophilic aromatic substitution; XRD, Powder X-ray diffraction.

* Corresponding authors.
E-mail addresses: sunhongfei@ctbu.edu.cn (H. Sun), shileichem@dlut.edu.cn (L. Shi).

https://doi.org/10.1016/j.arabjc.2024.105987
Received 29 May 2024; Accepted 2 September 2024
Available online 10 September 2024

and practical applications (*e.g.*, membrane separation, heterogeneous catalysis, rechargeable batteries, and smart sensing) (Liu et al., 2019b; Sun et al., 2020; Wang et al., 2020b; Zhi et al., 2020; Pourghasem et al., 2023; Tran et al., 2023). Especially for the COFs synthesis, significant breakthroughs have been witnessed in recent years, such as the acquisition of COF single-crystal (Evans et al., 2018; Han et al., 2024), the sp^2 carbon-conjugated COFs (Jin et al., 2017; Li 2021), the reconstruction synthesis methodology for highly crystalline COFs (Zhang et al., 2022b), COFs with weaving or catenane structures (Liu et al., 2016; Ma et al., 2023), and diverse ladder-type COFs (Zhi et al., 2022; Zhang et al., 2023b; Zhang et al., 2023c).

Ladder-type polymers are defined as multi-stranded polymers in which the backbones are linked by periodically repeated ring units via sharing two or more atoms (Che and Fang, 2020). In contrast to normal single-stranded polymers, the multi-stranded connecting mode ensures the good rigidity and remarkable chemical as well as thermal stability of polymer backbones. Especially for fully π-conjugated ladder-type polymers, the greatly extended π-conjugated length renders electron clouds could continuously delocalize along with the polymer backbone, providing significant convenience for the migration of electrons, excitons, and holes (Kitao et al., 2022). In earlier studies, researches on ladder-type polymers mainly focused on linear ladder polymers, such as linear PIMs for separation membranes and ladder-type conjugated arenes for photovoltaic or semiconductor devices (Wu et al., 2015; Zhu et al., 2019). Recently, ladder-type polymers have been successfully extended to the fields of two-dimensional and even three-dimensional polymers. Taking FANs for example, they comprise entirely π-conjugated ladder-type networks (Mahmood et al., 2019). The integration of the structural characteristics of different types of polymers has been a very meaningful approach to explore unprecedented new materials. Combining ladder polymers and COFs, the resultant ladder-type COFs would integrate both merits of them. The structural feature of ladder-type COFs is well illustrated in Fig. 1. Notably, it is necessary to clarify the differences between FANs and ladder-type COFs. Most importantly, FANs are amorphous with many linking defects in the polymer skeletons, while ladder-type COFs are well crystalline corresponding to less linking defects. In regard of chemical structure, both FANs and ladder-type COFs are double stranded, but FANs are fully conjugated structures that are usually connected by irreversible chemical bonds (Ahmad et al., 2020), while the skeletons of ladder-type COFs could be either conjugated or non-conjugated. It should be emphasized that the reversibility is not an absolute concept. For even the same chemical reaction, the degree of reversibility varies greatly upon different conditions, so it could provide either FAN or ladder-type COF depending on the reaction environments (Kim et al., 2018; Shehab et al., 2021). In particular, for monomers with large conjugated lengths, COFs could be also gained from irreversible reactions owing to the rigid structure, proper functional orientation, and strong intermolecular interaction. Logically, the distinction of FANs and the confirmation of the successful formation of ladder-type COFs are based on a variety of experimental and theoretical techniques, including Fourier transform infrared spectroscopy (FT-IR), solid-state cross-polarization/magic angle spinning ^{13}C nuclear magnetic resonance (CP/MAS ^{13}C NMR), powder X-ray diffraction (PXRD), BET surface area analysis, high resolution electron microscopy, and Materials Studio simulations.

Ladder-type COFs are initially designed to overcome the chemical stability and the shortcoming of lack intra-sheet π-conjugation in normal COFs. Although there are many challenges in the preparation of ladder-type COFs, such as low crystallinity, undesirable non-ladder defects and solubility problems, the unique ladder-type structures make them attractive for applications in various fields. Especially for fully π-conjugated ladder-type COFs, in addition to ordered holey graphene-like skeletons, they also usually contain various heteroatoms (*e.g.*, N, S, and O), both of which are meaningful for fundamental and application researches. Apart from these factors, together with the high design flexibility and the good manipulability of skeleton or porous features, ladder-type COFs show great promise for many useful fields, such as adsorption and separation (Guan et al., 2019; Cheng et al., 2021), sensing (Meng et al., 2019b; Yue et al., 2021b; Niu et al., 2022; Liu et al., 2024), photocatalysis (Gao et al., 2022; Zhi et al., 2022), and energy conversion and storage (Zhang et al., 2023b; Zhang et al., 2023c; Zou et al., 2023; Wang et al., 2024a; Yang et al., 2024). Accordingly, ladder-type COFs play increasingly important roles in diverse fields. Surprisingly, although there are a lot of literatures reviewing COFs (Xiao et al., 2023; Arora et al., 2024; Qin et al., 2024; Yao et al., 2024), no specific reviews focus attention on these unique ladder-type skeletons. Considering the booming trends in this field, as well as to inspire more chemists, physicists and material scientists to devote themselves to investigating these unique structures, this article systematically summarizes the rational design and synthesis of ladder-type COFs.

2. Topology design of ladder-type COFs

The multi-stranded linking mode in ladder-type COFs means that more repeating reactions occur during polymer preparation. Therefore, ladder-type COFs put forward higher requirements for the repeating linkages between building blocks. Generally, in addition to the good manipulation of reaction conditions, two more factors play crucial roles

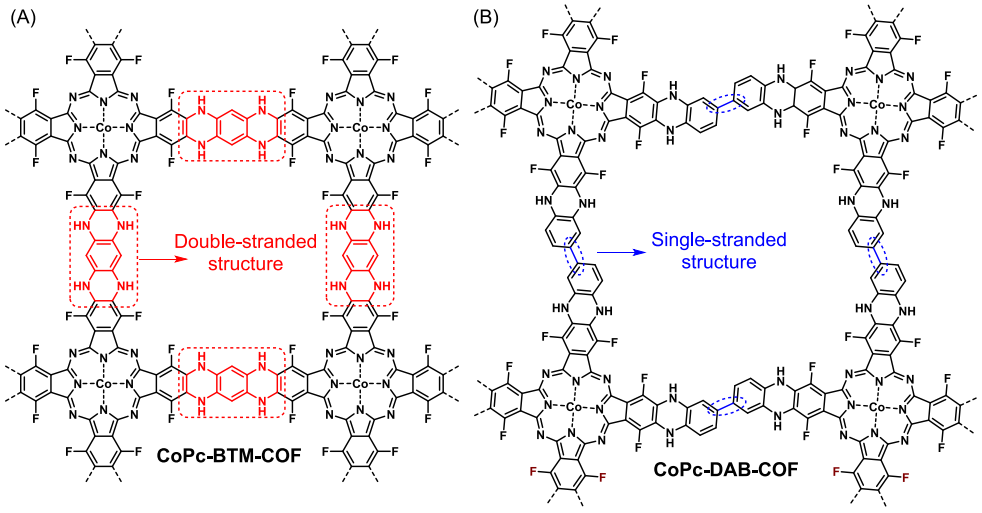

Fig. 1. Example of the comparison of the structural feature of different types of COFs: (A) ladder-type CoPc-BTM-COF with double-stranded linkers and (B) conventional CoPc-DAB-COF with single-stranded linkers.

in the formation of COFs: 1) the topological structure of functional groups in building blocks and 2) the number of functional groups and the chemical reactions between them. The topology of building block affects the orientation of functional groups and ensures that the linking units can form periodic structure and determine the size as well as the shape of final porous structure. The type of reaction and the conditions under which it occurs are crucial factors that determine both the efficiency and reversibility of the reaction. Among these conditions, topological feasibility is the prerequisite for preparing ladder-type COFs.

By virtue of the rich experience and computational techniques accumulated in the study of single-stranded connecting COFs, the rational molecular design for the preparation of ladder-type COFs has been achieved. Certainly, in comparison to single-stranded COFs bearing diverse topological structures (Liang and Zhao, 2018; Liang et al., 2020), only two-dimensional ladder-type COFs with high symmetries (*e.g.*, hexagonal and tetragonal pores, as shown in Fig. 2) have been reported. Generally, the hexagonal structure could be obtained by connecting C_3 + C_2 (Fig. 2A) or C_3 + C_3 (Fig. 2B) topological building blocks, the former of which usually yields a larger pore size. Similarly, the combination of C_4 + C_2 (Fig. 2C) or C_4 + C_4 (Fig. 2D) topologies produce a tetragonal skeleton. For some special polymers (*e.g.*, polymetallophthalocyanine), the tetragonal framework could be obtained through individual C_2 monomer (Fig. 2E). Undoubtedly, a smaller monomer size would lead to a smaller pore size of framework for this methodology since only part of molecular structure act as the linking units between building blocks. Compared to a variety of topologies of monomers for single-stranded COFs, only C_2, C_3 and C_4 topological monomers are reported. On one hand, a simple topological structure is conducive to the formation of high crystalline polymers. On the other hand, more complex topologies will encounter great challenges in monomer and polymer synthesis. Fig. 3 illustrates the common reported monomers bearing different topological structures and different functional groups for constructing ladder-type COFs. In addition to the large conjugated size and the rigid molecular skeleton, the orientation of functional groups keeps highly consistent, and all of these factors are favorable for the formation of ladder-type COFs.

3. Synthesis of ladder-type COFs

Depending on the different features of organic reactions, many linkages have been utilized to construct COFs with single-stranded linkages, including boroxine, boronate ester, triazine, imine, hydrazone, azine, imide, amide, urea, and C═C double bond (Geng et al., 2020b). In consideration of the multi-stranded (mostly double-stranded) connecting modes in ladder-type COFs, most of these reactions don't work anymore. Fig. 4 lists the common reported reactions applied to construct ladder-type COFs. According to different reaction methods, this section will detailedly discuss how to reasonably select monomers with different functional groups as well as different topological structures and how to optimize the reaction conditions to gain the desired ladder-type COFs.

3.1. Condensation reaction

3.1.1. Condensation reaction of diketone and diamine

The reaction between aromatic amine and aromatic aldehyde has been an effective approach to produce single-stranded COFs, the resultant linkages of which are generally Schiff-base (*e.g.*, imine, hydrazone, and azine) or β-ketoamine (Segura et al., 2016). Stimulated by these examples, replacing aldehyde with diketone, Guo (Guo et al., 2013) successfully synthesized the first ladder-type COFs (CS-COF in Fig. 5) with pyrazine as the connecting units. In their study, *tert*-butylpyrene tetraone (M1 in Fig. 3) and triphenylene hexamine (M5 in Fig. 3) with C_2- and C_3-symmetry, respectively, were selected as two key building blocks (synthesis information is summarized in Table 1). The CS-COF was isolated with a high yield (90 %) under solvothermal conditions in strong polar mixed solvent, and the crystalline COF structure was reasonably demonstrated by various techniques. Nitrogen sorption isotherm curves showed that the BET surface area of CS-COF was as high as 776 $m^2\ g^{-1}$. In contrast to the sensitive stability of conventional COFs upon acid or base conditions, the CS-COF structure remained nearly intact in various organic solvents with different polarity, aqueous NaOH or HCl solutions (1 M), indicating the good chemical stability of the double-stranded ladder skeleton. The effects of *tert*-butyl groups are supposed to be double-edged: on one hand, they are helpful to enhance the solubility of monomer; on the other hand, the presence of *tert*-butyl motifs interferes with the interactions between COF layers, leading to a slipped AA-stacking mode and decreased crystalline particles.

In order to circumvent the complicated, dangerous and tedious synthesis procedures (such as sealing, strong acid/base, high

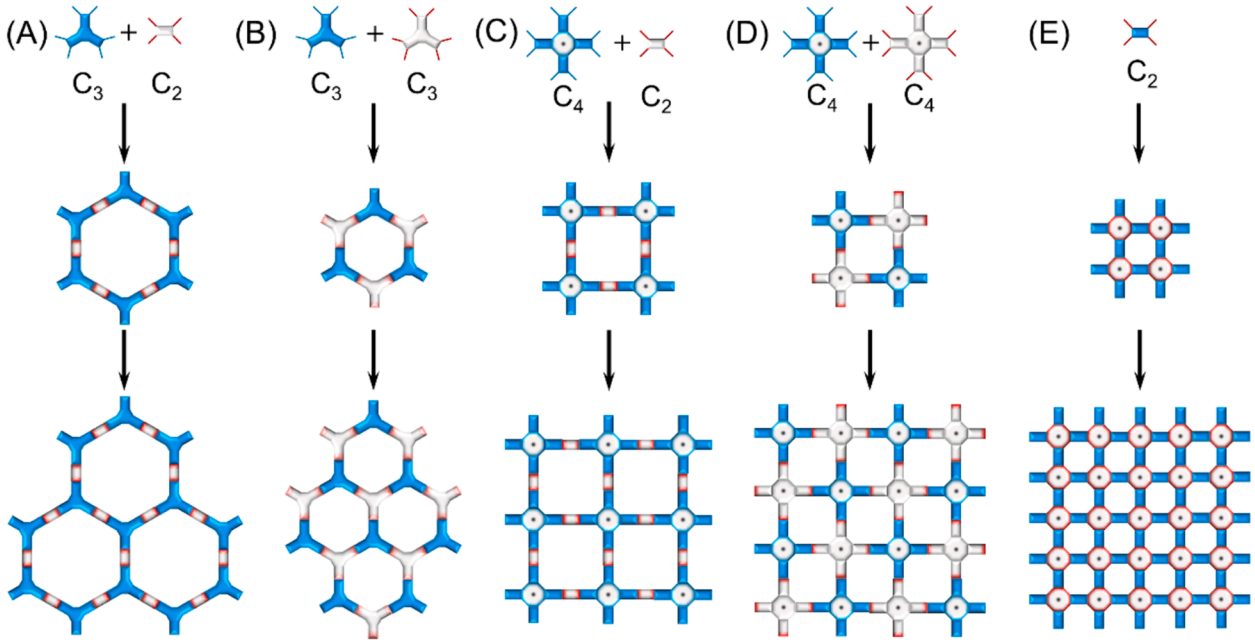

Fig. 2. Topological illustrations exhibiting the reported connecting modes of building blocks bearing different symmetries applied to construct ladder-type COFs.

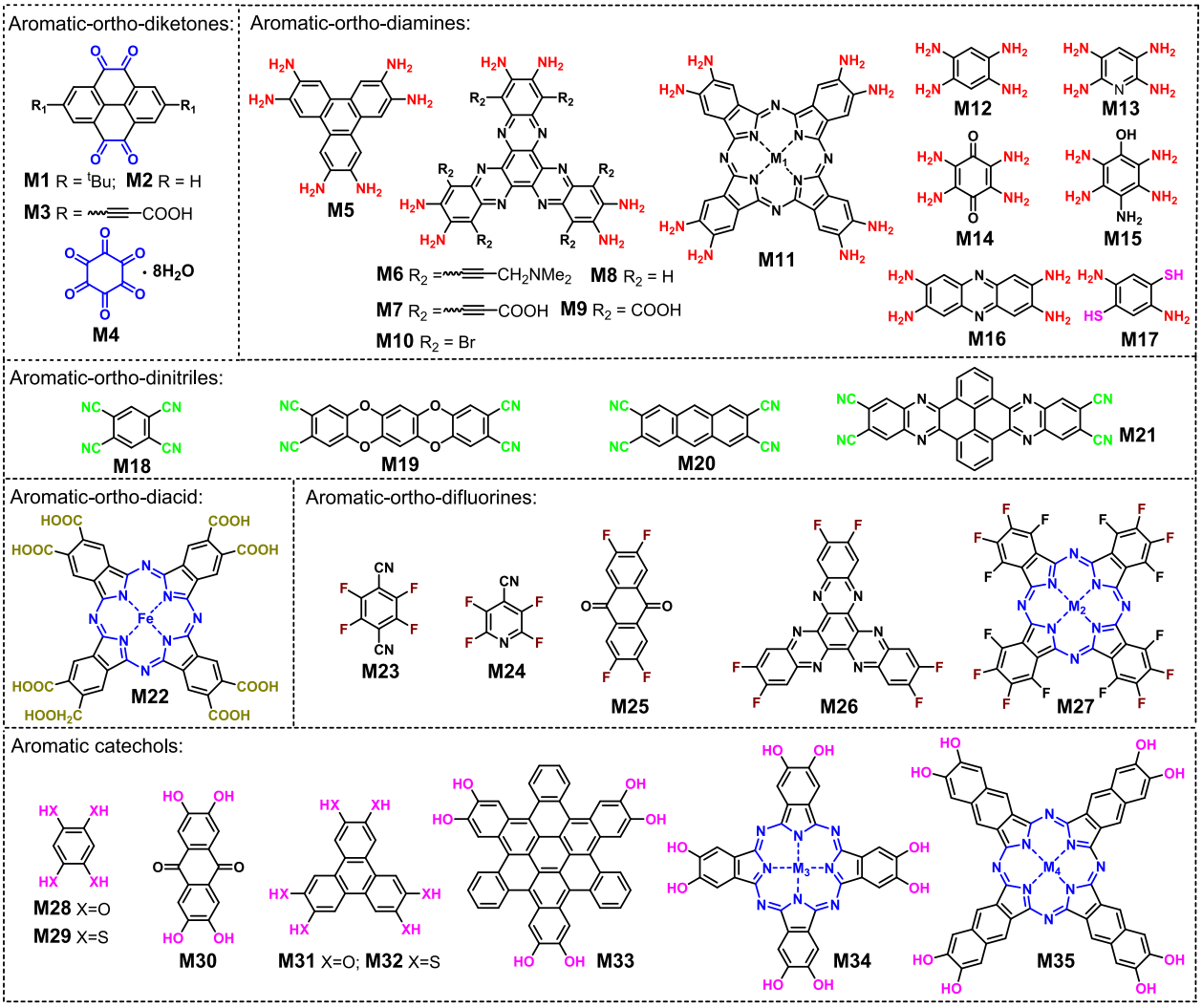

Fig. 3. Monomers bearing different functional groups for constructing ladder-type COFs.

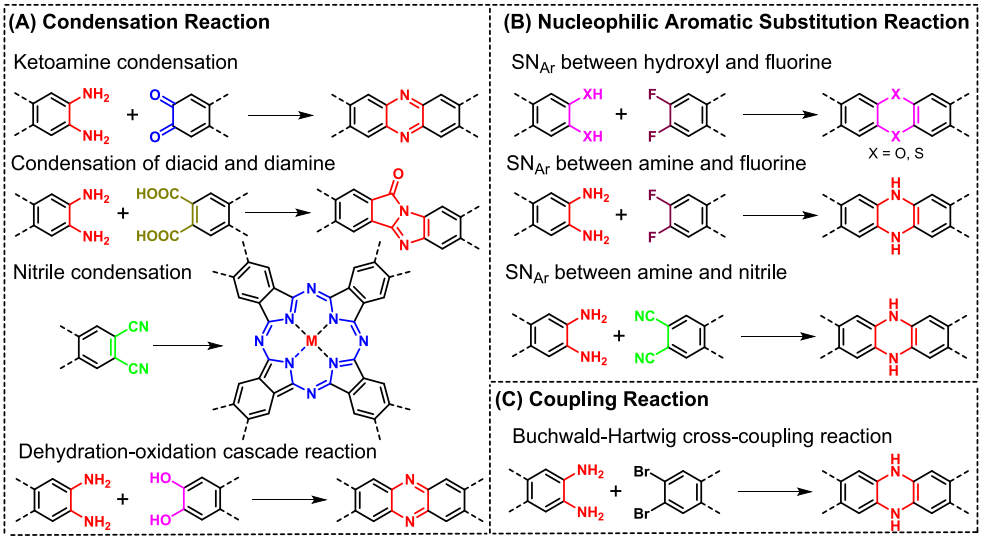

Fig. 4. Common reported organic reactions applied to construct ladder-type COFs: (A) condensation reactions, (B) nucleophilic aromatic substitution reactions, and (C) coupling reaction.

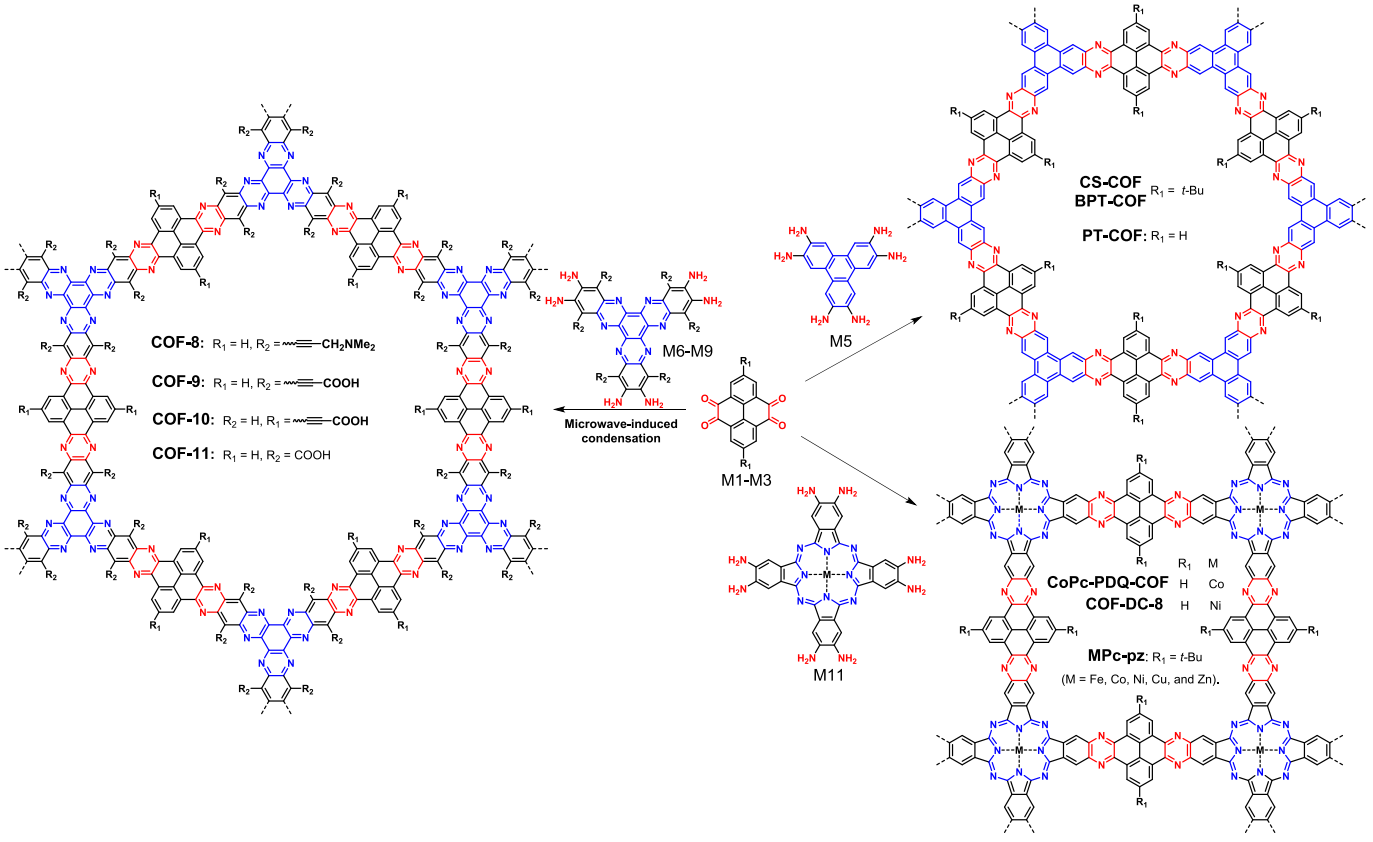

Fig. 5. Synthesis of fully π-conjugated ladder-type COFs via condensation reaction of pyrene-4,5,9,10-tetraone derivates and aromatic amines.

temperature, and high pressure) using solvothermal reactions, Bai (Bai et al., 2022) developed a facile liquid-phase method to synthesize BPT-COF (structure sees Fig. 5, the same skeleton as CS-COF). For the novel method, M1 (0.06 mmol) and M5 (0.04 mmol) was dissolved in acid/o-dichlorobenzene (200 mL/200 mL) and water (200 mL) to form dilute solutions, respectively. After sonicating for 15 min, the organic phase was added dropwise into the aqueous solution at room temperature. The mixture was stirred under ambient atmosphere until the system reached equilibrium (about 24 h) indicated by XRD and dynamic light scattering (DLS). After filtration and Soxhlet extraction, the resultant BPT-COF was subsequently confirmed to be high-quality COF. Given the great convenience of this technology, it was also successfully conducted to synthesize PT-COF which could not be prepared through normal solvothermal method owing to the solubility problem of M2. As illustrated in Fig. 6, in contrast to conventional solvothermal method, it is supposed that the liquid-phase method realizes the direct nucleation and growth of high-quality COFs and avoids the need for the formation of polygonal sheets as well as complicated crystallization process.

Using pyrene-4,5,9,10-tetraone derivates (M2 and M3 in Fig. 3) as the core of *ortho*-diketone, Hoberg research group (Kuehl et al., 2018; Duong et al., 2019) designed and prepared a series of ladder-type COFs (COF8–COF11 in Fig. 5) with hexaazatrinaphthalene (HATN) as the core of aromatic *ortho*-diamine (M6–M9 in Fig. 3). In contrast to triphenylene, HATN derivatives are more synthetically available and are provided with larger molecular sizes, and therefore the functionalization of COFs as well as the regulation of pore size (1.9–2.8 nm) become more convenient (Wang et al., 2022; Weng et al., 2022). Microwave-induced condensation approach was also applied to prepare these COFs in their study (Table 1 entry 3), and it was supposed that the enhanced material–microwave interactions would favor the crystal growth during polymerization process. Successfully, positive (M6), negative (M7), and neutral (M8) monomers were all proved to be able to proceed polymerization smoothly, providing a significant chance for regulating the interactions between the COFs and different guest molecules.

Except for the "3+2" synthetic strategy to yield hexagonal topology, metallophthalocyanines (M11 in Fig. 3) bearing C_4 symmetry was also chosen as planar conjugated building blocks to give tetragonal skeletons. Metallophthalocyanine has large conjugation length and strong intermolecular interaction, making it possible to synthesize COFs with higher conductivity. In addition, nitrogen-rich skeleton and tunable central metal atoms endow the corresponding COF materials with good recognition and catalytic properties. Several independent research groups have synthesized different ladder-type COFs based on M11, including Huang (Huang et al., 2020a), Wang (Wang et al., 2019), Zhang (Zhang et al., 2020a), and Meng (Meng et al., 2019b). The solvothermal method was mostly applied to prepare these COFs, and microwave heating was found to be useful to reduce the reaction time (from several days to 10 h), but it would slightly diminish crystallinity (Meng et al., 2019b). Recently, Zhong (Zhong et al., 2021) found the highly soluble and oxidatively stable *ortho*-diphenylmethanimine-substituted metallophthalocyanine monomers ($MPc(N{=}CPh_2)_8$) are beneficial to improve the crystallinity of COF (FePc-pz in Table 1 entry 6), and water also plays an essential role in promoting the reaction equilibrium during polymerization. Several non-noble metal elements (*e.g.*, Fe, Co, Ni, Cu, and Zn) were successfully incorporated into these ladder-type COFs using $MPc(N{=}CPh_2)_8$ as precursors, some of which couldn't be prepared by the direct condensation from M1 and M11.

Hexaketocyclohexane (M4 in Fig. 3), bearing C_6-symmetry, represents another important building block that could react with aromatic-*ortho*-diamine to yield pyrazine linkage, resulting in hexaazatriphenylene (HAT) or HATN as the fundamental cores of ladder-type COFs. Although M4 is a C_6-symmetric monomer, it consumes two adjacent ketone functional groups simultaneously in the preparation of ladder-type polymers, so it can also be treated as a C_3-symmetric monomer if two adjacent ketones were viewed as a whole chromophore. As a matter of fact, gaining ladder-type COFs from M4 is a very tricky

Table 1
Selected examples of the synthesis of ladder-Type COFs.

Entry	COFs	Monomers	Reaction Method	Reaction type	Functional groups of monomers	Stacking mode	Pores [nm]	S_{BET} [m^2/g]	Ref.
1	CS-COF	M1, M5	solvothermal	condensation	ketone, amine	slipped AA	1.6	776	(Guo et al., 2013)
2	BPT-COF	M1, M5	liquid-phase	condensation	ketone, amine	AA	1.6	184	(Bai et al., 2022)
3	COF8	M2, M6	microwave	condensation	ketone, amine	/	/	/	(Kuehl et al., 2018)
4	CoPc-PDQ-COF	M2, M11	solvothermal	condensation	ketone, amine	AA	2.2	762	(Huang et al., 2020a)
5	NiPc-COF	M1, M11	solvothermal	condensation	ketone, amine	slipped AA	1.3–2.1	358	(Zhang et al., 2020a)
6	FePc-pz	M1, FePc $(N{=}CPh_2)_8$	solvothermal	condensation	ketone, amine	serrated AA	1.8–3.8	290	(Zhong et al., 2021)
7	aza-COF-2	M4, M12	solvothermal	condensation	ketone, amine	AA	1.41	102	(Meng et al., 2019a)
8	PGF-1	M4, M12	solvothermal	condensation	ketone, amine	AA	1.12	101	(Li et al., 2020)
9	HAQ-COF	M4, M14	solvothermal	condensation	ketone, amine	inclined stacking	/	53	(Wang et al., 2021)
10	TQBQ-COF	M4, M14	solvothermal	condensation	ketone, amine	AB	1.18	94	(Shi et al., 2020)
11	F-COF	M4, M15	solvothermal	condensation	ketone, amine	AA	/	/	(Mahmood et al., 2020)
12	PA-COF	M4, M16	solvothermal	condensation	ketone, amine	AA	2–5	19.6	(Wang et al., 2020a)
13	aza-COF-1	M4, M5	solvothermal	condensation	ketone, amine	AA	0.99	99	(Meng et al., 2019a)
14	COF_{BTC}	M17	Microwave	condensation	nitrile	AA	/	/	(Peng et al., 2019)
15	CuPc-2D-cCOF	M17	ionothermal	condensation	nitrile	AA	0.8	/	(Yang et al., 2022b)
16	QPP-FAC-Pc-COF	M21	ionothermal	condensation	nitrile	AA	1.6–2.0	350	(Yang et al., 2022a)
17	Cu-anPPC	M20	ionothermal	condensation	nitrile	AA	0.5, 0.9	2043	(Seob et al., 2023)
18	FePc-BBL	M22, M14	solvothermal	condensation	carboxyl, amine	AB	/	29	(Zhang et al., 2022c)
19	PZ-COF-1	M31, M12	solvothermal	condensation	hydroxyl, amine	AA	1.8	845	(Ma et al., 2019)
20	HHTP-TABQ	M31, M14	solvothermal	condensation	hydroxyl, amine	AA	2.43	37.5	(Zhang et al., 2023a)
21	JUC-505	M31, M23	solvothermal	S_NAr	hydroxyl, fluorine	AA	1.68	1584	(Guan et al., 2019)
22	COF-318	M31, M24	solvothermal	S_NAr	hydroxyl, fluorine	AA	1.5	576	(Zhang et al., 2018)
23	TH-COF	M31, M24	microwave	S_NAr	hydroxyl, fluorine	AA	2.2	1254	(Ji et al., 2020)
24	NiPc-TFPN	M34, M23	solvothermal	S_NAr	hydroxyl, fluorine	AA	1.2	252	(Lu et al., 2021)
25	CoPc-O-COF	M28, M27	solvothermal	S_NAr	hydroxyl, fluorine	AA	1.7	183	(Zhi et al., 2024)
26	$CuPcF_8$-CoPc-COF	M34, M27	solvothermal	S_NAr	hydroxyl, fluorine	AA	1.0	376	(Yue et al., 2021a)
27	CoPc-BTM-COF	M12, M27	solvothermal	S_NAr	amine, fluorine	AA	1.7	192	(Zhi et al., 2022)
28	NiPc-NH-$CoPcF_8$	M11, M27	solvothermal	S_NAr	amine, fluorine	AA	1.0	209	(Yue et al., 2022)
29	COF-4	HAT-CN, M12	solvothermal	S_NAr	nitrile, amine	/	/	/	(Kuehl et al., 2021)
30	PTHAT-COF	HAT-CN, M13	solvothermal	S_NAr	nitrile, amine	/	3	65.71	(Wang et al., 2024a)
31	PTDCOF	M5, HBTP	solvothermal	coupling reaction	amine, bromine	AA and AB	1.1	32.6	(Zhou et al., 2021)

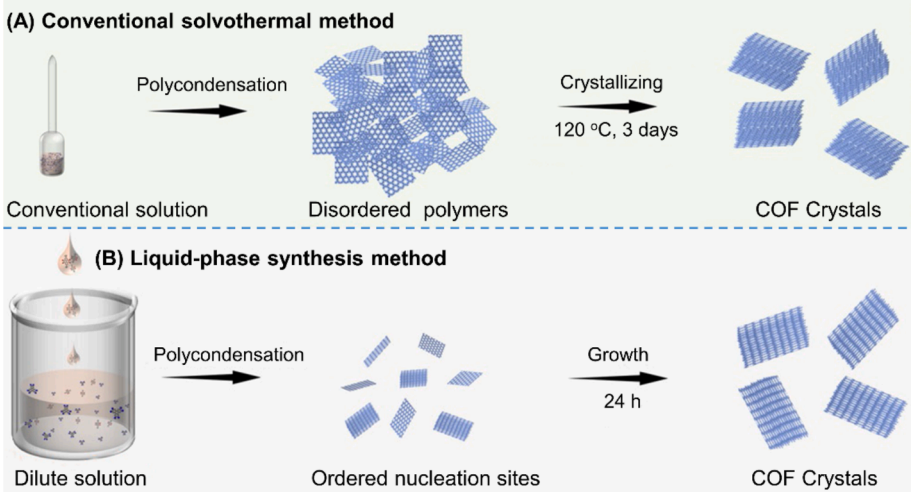

Fig. 6. Schematic representation of the difference between solvothermal method and liquid-phase synthesis in the formation of aza-COFs (Bai et al., 2022).

job. Taking M4 and 1,2,4,5-benzenetetramine (M12 in Fig. 3) as an example, the condensation reaction usually results in amorphous CMPs (Wang et al., 2022; Weng et al., 2022). It was not until 2019 that Meng (Meng et al., 2019a) successfully prepared ladder-type COFs (aza-COF-2 in Fig. 7) using M4 and M12 via a solvothermal method with NMP and concentrated sulfuric acid as solvent and catalyst, respectively. The main reason for the difficulty in preparing ladder-type COFs could be attributed to the poor reaction reversibility in the formation of pyrazine, leading to nonspecific reactive sites and mishaps of connectivity. In 2020, Li (Li et al., 2020) found that operating the reaction under basic aqueous conditions would improve the dynamic reversibility of the reaction, facilitating the growth of crystalline frameworks. From then on, various C_2-symmetric aromatic-*ortho*-diamines were successively selected to react with M4 to give ladder-type COFs (Table 1 entries

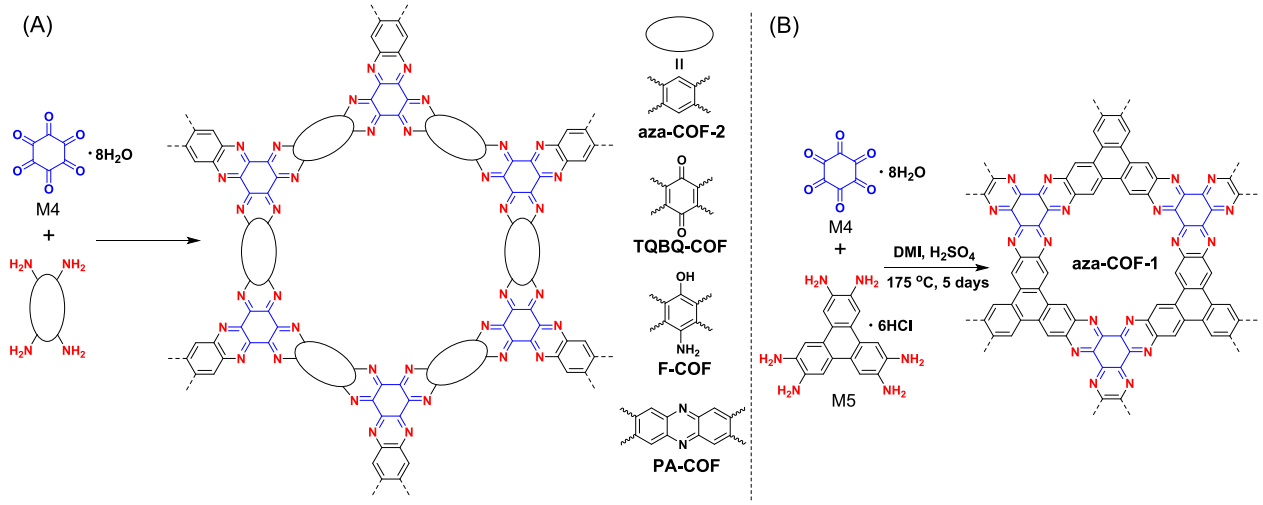

Fig. 7. Synthesis of fully π-conjugated ladder-type COFs via condensation reaction of hexaketocyclohexane and aromatic amines.

9–12). As illustrated in Fig. 3 and Fig. 7, M14 containing quinone functional groups is provided with strong electrochemical activity (Shi et al., 2020; Zhang et al., 2023b), and M15 makes the resultant COF bear highly polar amine and hydroxyl groups (Mahmood et al., 2020), and M16 has a larger molecular size and is also a redox-active moiety (Wang et al., 2020a; Parvatkar et al., 2023). Certainly, M4 could also react with aromatic amines with C_3-symmetry. Nevertheless, owing to the limited selection of proper monomers with C_3-symmetry, only M5 was attempted to react with M4 (Fig. 7B) (Meng et al., 2019a; Yang et al., 2019; Xie et al., 2022). We think the combination of M4 with the above mentioned HATN-based amines (M6–M9) might be a very good choice, the resulting nitrogen-rich aza-fused frameworks would present task-specific applications in photocatalytic and electrocatalytic fields (Chen et al., 2022; Weng et al., 2022).

Due to the significant differences in chemical composition, conjugation size and topological structure between different monomers, the layer-layer stacking mode of COFs layer varies a lot. For COFs based on pyrene-4,5,9,10-tetraone derivates, AA eclipsed structure is often probed since large conjugation length of repeating units leads to intensive π-π stacking interaction. Taking CoPc-PDQ-COF (structure sees Fig. 5) as example, the assignment of the stacking manner, the differences in the AA and AB stacking styles, and the multidirectional views of the AA stacking mode are well outlined in Fig. 8. M1 related COFs mostly present slipped or serrated AA-stacking mode because of the steric hindrance effect of *tert*-butyl groups. For M4-based COFs, the stacking modes are chiefly determined by amine monomers. Generally, COFs gained from M12 and M16 monomers adopt AA eclipsed conformation, and M14-based COFs stack in staggered AB-stacking style owing to the electrostatic repulsion of the carbonyl groups. For the BET surface area of COFs, in comparison to those of the COFs gained from M1–M3, the BET surface areas of the COFs stemmed from M4 are much lower, most of which were lower than 100 m^2/g. The reason might be ascribed to the small molecular size of M4. The functional groups are too close together to each other, affecting the reactivity of remaining functional groups after two or four carbonyl groups being consumed and leading to more defects. Moreover, the interlayer repulsion originated from the more polarized imine groups would also exert influence on the compact packing between COF layers (Wang et al., 2022). How to synthesize ladder-type COFs bearing high crystallinity and high BET surface area simultaneously from M4 monomer is a very challenging and attractive task.

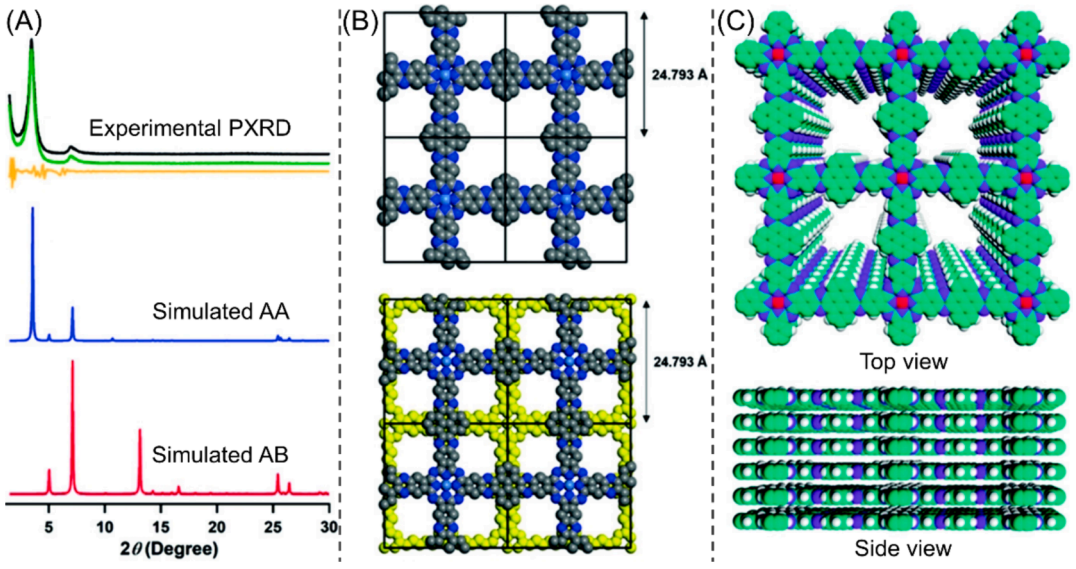

Fig. 8. (A) Experimentally observed PXRD and simulated XRD profiles of CoPc-PDQ-COF, (B) simulated AA and AB stacking style of CoPc-PDQ-COF, and (C) top and side views of the simulated AA stacking manner of CoPc-PDQ-COF (Huang et al., 2020a).

3.1.2. Tetramerization of nitriles

Nitrile group can be transformed into various structures under different conditions, and it has been widely used for constructing covalent triazine frameworks, in which three nitriles are condensed to a triazine ring linked by C—C single bond with other subunits (Zhang and Jin, 2018; Liu et al., 2019a; Tahir et al., 2019). For aromatic-*ortho*-dinitrile derivatives, they can be condensed into graphitic carbon nitride materials at high temperature (*e.g.*, 550–700 °C), such as the pyrolysis of hexaazatriphenylene–hexacarbonitrile (HAT-CN) to give C_2N material (Walczak et al., 2018). More specifically, they could be also condensed to polymetallophthalocyanine at proper temperature (usually below 500 °C) in the presence of catalyst (*e.g.*, 1,8-diazabicyclo(5,4,0)undec-7-ene, DBU) or metal salts (Chen et al., 2019). Remarkably, ladder-type metallophthalocyanine-based COFs could be prepared under suitable polymerization conditions. Peng (Peng et al., 2019) prepared the first ladder-type metallophthalocyanine-based COFs (Fig. 9A). In their study, $FeCl_3$ was introduced since the empty d orbitals in iron atomic orbitals have strong coordination ability to the nitrogen atom of nitrile group, thus it can serve as a structure direction agent to promote the tetramerization cyclization of nitrile groups and the construction of fully conjugated polyphthalocyanine framework. With 1,2,4,5-tetracyanobenzene (M18 in Fig. 3) and DBU acting as monomer and catalyst, respectively, a relatively efficient and mild microwave irradiation method was applied instead of traditional solvothermal method to prepare COF_{BTC}. Specifically, the crystal structures of COF_{BTC} were resolved to a combination of orthorhombic AA stacking and hexagonal AA stacking via PXRD, high-angle-annular-dark-field scanning transmission electron microscopy, and theoretical simulations (Fig. 9B). Furthermore, in view of the charged center of polymetallophthalocyanine, hydroxyl groups could incorporate into the stacking layers and absorb onto the positively charged metal centers. Therefore, COF_{BTC} showed good solubility upon strong alkaline conditions owing to electrostatic repulsion after the adsorption of OH^-. Under similar synthetic conditions but with different metal salts ($TiCl_4$, $CuCl_2{\cdot}2H_2O$ or $CoCl_2{\cdot}6H_2O$), different polymetallophthalocyanine COFs (MPc-COF, M = Ti, Cu, or Co) were also successfully prepared (Jiang et al., 2022; Liu et al., 2022).

To alleviate the utilization of toxic solvents as well as the small-dose synthesis issue in the microwave-assisted synthesis method, Yang (Yang et al., 2022b) developed an ionothermal synthesis approach to prepare these fully conjugated COFs (MPc-2D-cCOFs in Fig. 10, the same framework skeleton as COF_{BTC}). Indeed, the reaction temperature (350 °C) was higher than the boiling point of M18 (268 °C), and the polymerization speed was obviously accelerated when the temperature exceeded the boiling point of M18, implying the dual roles of M18 as both a monomer and a high boiling solvent. Using ionothermal synthesis method, monomers with more flexible structure (M19 in Fig. 10) or greater conjugation length (M21 in Fig. 10) were successfully conducted to facilitate electron transport and electrolyte transportation in potassium-ion batteries (Yang et al., 2022a; Seob et al., 2023).

In addition to the polymerization method, Zhang (Zhang et al., 2023c) paid close attention to the central metal atoms of polymetallophthalocyanine COFs since the actual crystallinity of COFs depends highly on the metal source. Metallic powders (Fe or Co) and metal salts ($NiCl_2$ or $CuCl_2$) were selected as different metal sources for the ionothermal synthesis of different COFs containing various central metal atoms. Interestingly, the resulting *p*MPc COFs were found to have different metal contents, in which the metal contents of *p*FePc (6.44 %),

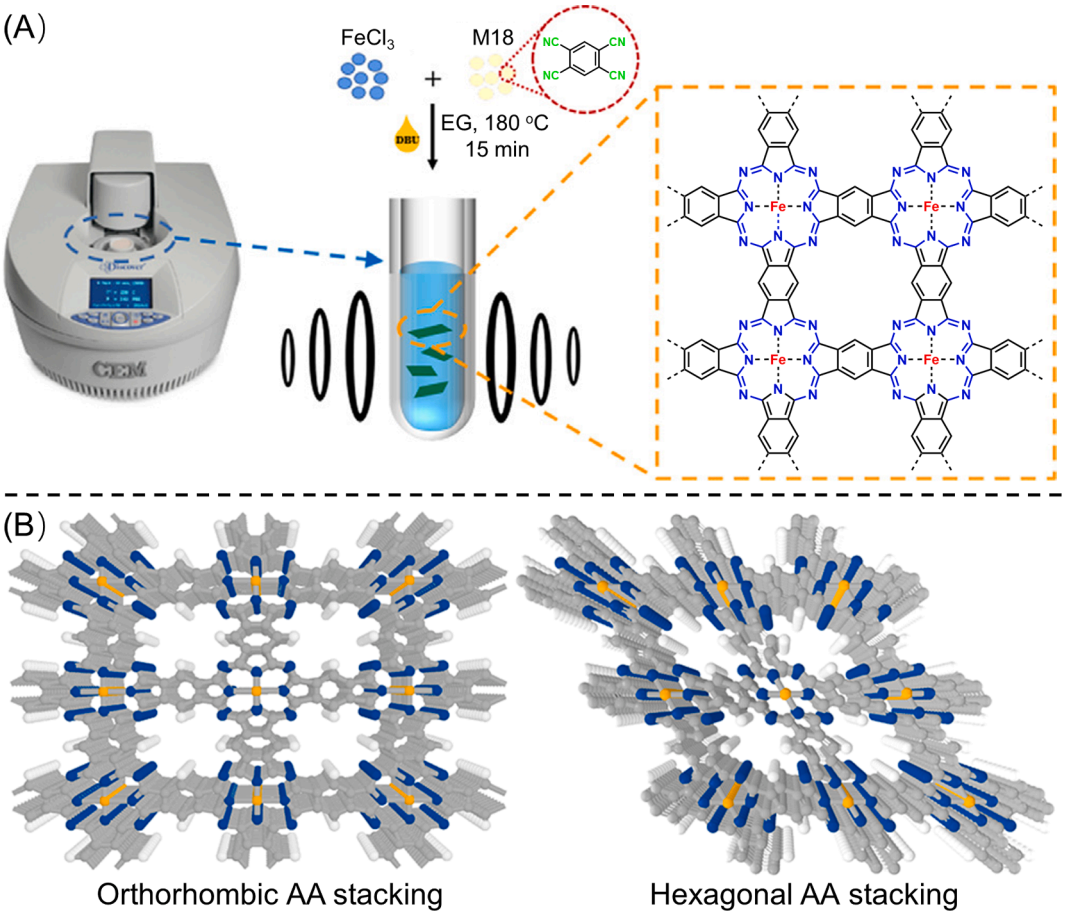

Fig. 9. (A) Schematic representation for the synthesis of COF_{BTC} and (B) reconstructed models of COF_{BTC} for orthorhombic and hexagonal stacking manners (Peng et al., 2019).

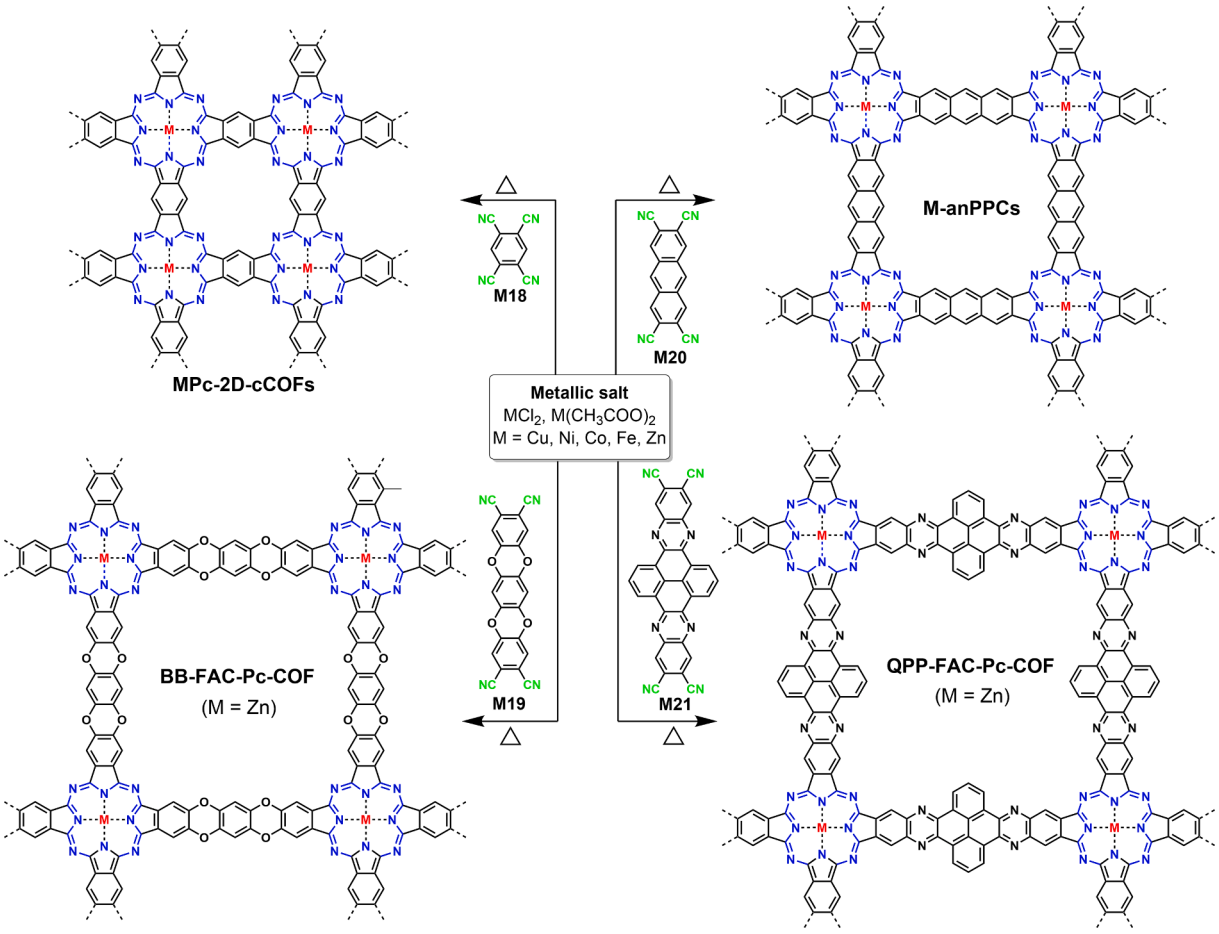

Fig. 10. Schematic diagram of COFs synthesized from the tetramerization of nitriles using ionothermal synthesis method.

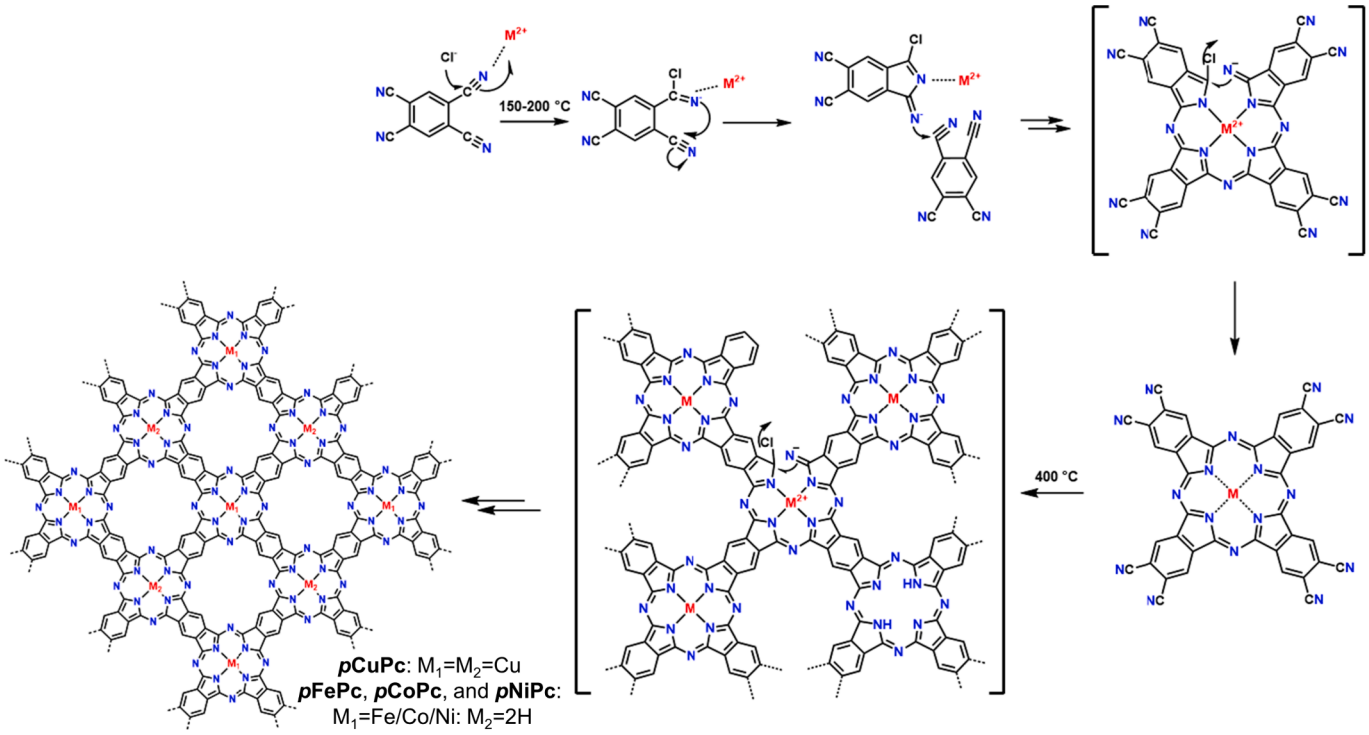

Fig. 11. Proposed mechanism for the formation of polymetallophthalocyanine by ionothermal method via two critical steps: the formation of octacyanophthalocyanine intermediate followed by the subsequent polymerization (Zhang et al., 2023c).

*p*CoPc (6.70 %), and *p*NiPc (7.31 %) were nearly half of *p*CuPc (13.26 %). Two critical steps in polymerization and two types of configurations were supposed to explain this phenomenon. As displayed in Fig. 11, 1,2,4,5-tetracyanobenzene was firstly condensed to octacyanophthalocyanine intermediate, and *p*FePc, *p*CoPc, and *p*NiPc were formed from alternatively fused MPc and Pc subunits, while *p*CuPc was fused solely with the CuPc subunit. Focus on the central metal ions, Song (Song et al., 2023) incorporated different metal atoms into polymetallophthalocyanine via a mixed-metal ionothermal synthesis method to regulate charge interactions between different metallophthalocyanine centers. Equimolar MCl_2 (M = Cu, Ni, Co, and Fe) was mixed with $ZnCl_2$ as both metal sources and high boiling solvent for ionothermal synthesis, and the resulting COFs (M-anPPC in Fig. 10) would have different metal contents as the different Irving–Williams series (Fe^{2+} < Co^{2+} < Zn^{2+} < Ni^{2+} < Cu^{2+}) of metal ions caused different coordination stability. Significantly, the BET surface area of Cu-anPPC (Table 1 entry 17) was as high as 2403 $m^2\ g^{-1}$, which is the highest value for porphyrin- and phthalocyanine-based POPs.

Based on the large conjugated structure of metallophthalocyanine and strong intermolecular interactions, most of the above mentioned polymetallophthalocyanine COFs show AA stacking configuration. Analogously, for different monomers or different polymerization methods, the BET surface areas of COFs make a big difference (from 9.31 $m^2\ g^{-1}$ to 2043 $m^2\ g^{-1}$), meaning the importance of operating conditions. Generally speaking, the BET surface areas of COFs stemmed from ionothermal synthesis are larger than those of microwave-assisted synthesis. By the way, polymetallophthalocyanine could also be prepared by reacting pyromellitic dianhydride (PMDA) with urea at high temperature, but only amorphous conjugated networks were produced (Yang et al., 2020; He et al., 2022; Pan et al., 2022).

3.1.3. Condensation of diacid and diamine

The combination of aromatic-*ortho*-diacid (or aromatic dianhydride) with aromatic monoamine would give aromatic polyimides. However, the condensation of aromatic-*ortho*-diacid (or aromatic dianhydride) and equivalent aromatic-*ortho*-diamine yields a new type of ladder-type polymer with fused benzimidazobenophenanthroline (BBL) motifs as linkages (Fig. 12A) (Shin et al., 2019; Noh et al., 2020; Yu et al., 2022b; Wang et al., 2023). The BBL functional group is a rigid double-stranded ladder structure composed of imide and imine, and the fully-conjugated linking mode provides the corresponding polymers with excellent chemical as well as thermal stability, outstanding optical and electronic features. Due to the low solubility of monomers as well as the low reaction reversibility of imide reaction, it is difficult to synthesize polyimide COFs (Zhang et al., 2020b), making it harder to prepare BBL-based COFs bearing rigid ladder-type linkage. Until recently, Zhang (Zhang et al., 2022c) reported the BBL-based ladder-type COF (FePc-BBL in Fig. 12B) via the condensation reaction of M22 and M14 under solvothermal conditions. In light of FePc-BBL has diverse polar functional groups and heteroatoms (*e.g.*, N and O), the charge repulsion between different layers renders FePc-BBL to show AB stacking mode, and the BET surface area is also undervalued to 29 m^2/g.

3.1.4. Dehydration-oxidation of amine and hydroxyl groups

Apart from the condensation of aromatic-*ortho*-diamine and aromatic-*ortho*-diketone, the pyrazine-linked COFs could be also prepared via aromatic-*ortho*-diamine and aromatic catechol derivatives. Different from ketoamine condensation, the new preparation method sometimes requires the presence of oxidizing agent. The actual reaction process is complicated, and it is indeed one-pot dehydration and oxidation tandem reaction, that is two reactions occur simultaneously. The reaction can proceed in two ways including dehydration/oxidation route and oxidation/dehydration route. For the dehydration/oxidation route (Fig. 13A), the aromatic amine dehydrates with the hydroxyl groups to give dihydrophenazine, and then it is further oxidized to phenazine. In regard of the oxidation/dehydration route (Fig. 13B), aromatic catechol is firstly oxidized to quinone intermediates, and then it occurs ketoamine condensation with aromatic amine. No matter which reaction comes first, the final products both result in phenazine.

In 2019, Ma (Ma et al., 2019) firstly reported the preparation of ladder-type COF (PZ-COF-1 in Fig. 13) using this tandem reaction strategy using M31 and M12 as monomers. The polymerization reaction was carried out in a mixed solvent with AcOH and $K_2Cr_2O_7$ as catalyst and oxidizer, respectively. PZ-COF-1 was highly crystalline with a high BET surface area of 845 m^2/g. In 2020, with O_2 as oxidizer, Jhulki (Jhulki et al., 2020) investigated the reaction mechanism of M31 and M5 by virtue of electron paramagnetic resonance (EPR) and mass spectrometry techniques. It was found that the reaction probably proceeded through the initial oxidation of M31 to quinone intermediates. Unfortunately, they did not get the desired COF materials. In 2022, Zhang

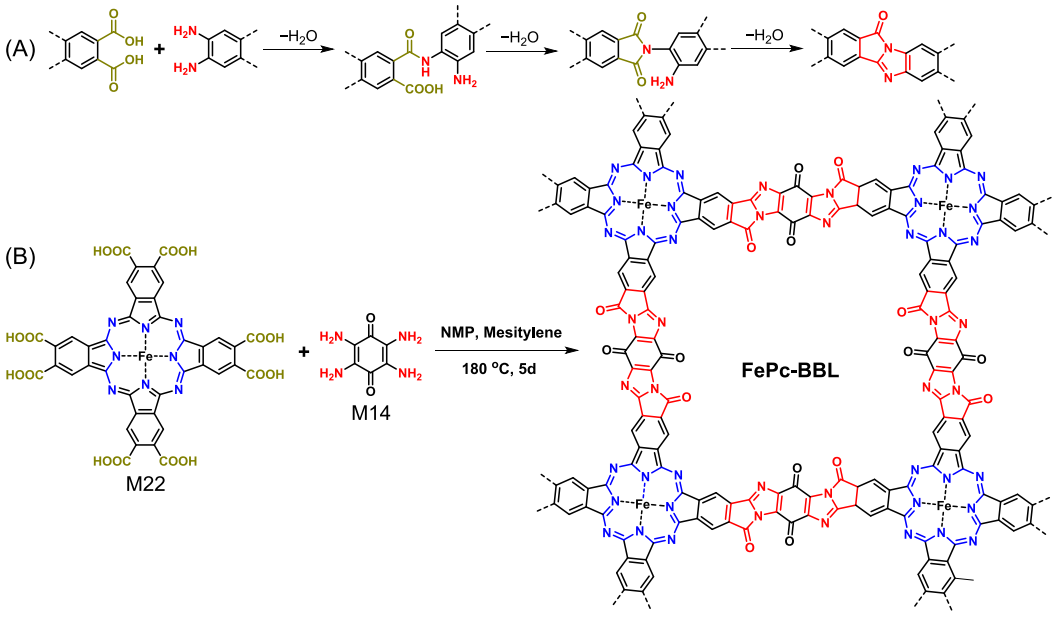

Fig. 12. (A) Formation of BBL from equivalent aromatic-*ortho*-diacid and aromatic-*ortho*-diamine and (B) synthesis of FePc-BBL COF through the condensation of aromatic diacid and diamine.

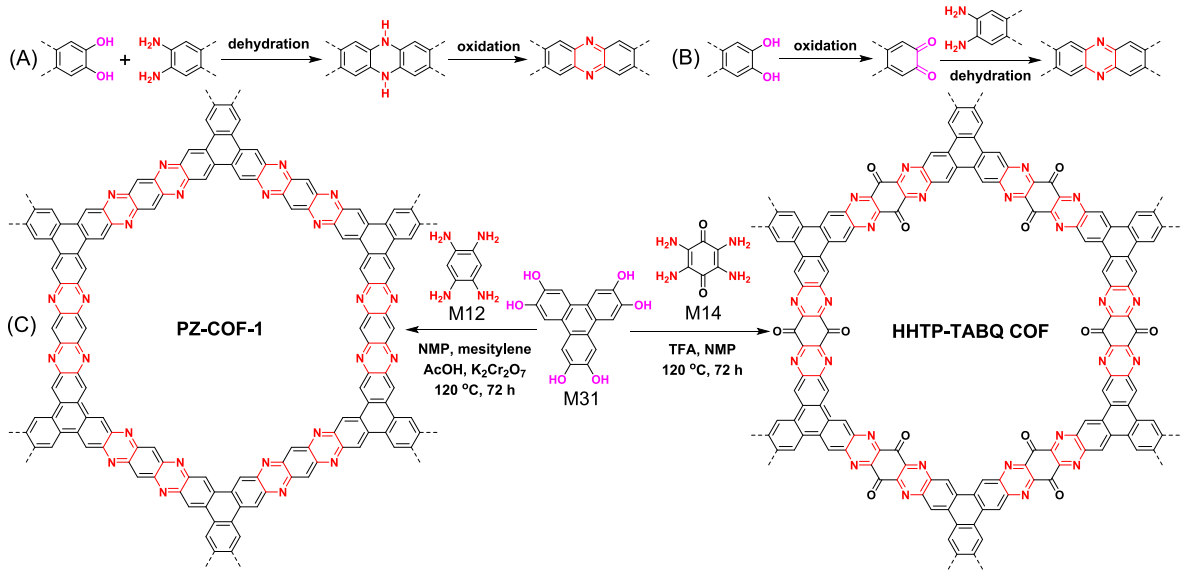

Fig. 13. Two potential ways to generate pyrazine linker from aromatic catechol and aromatic-*ortho*-diamine derivatives: (A) dehydration followed by oxidation route and (B) oxidation followed by dehydration route. (C) Examples of the synthesis of fully conjugated ladder-type COFs via dehydration/oxidation tandem reactions between amine and hydroxyl groups.

(Zhang et al., 2022a) successfully synthesized the desired COF using M31 and M5 via initial oxidation followed by a dehydration strategy. M31 was firstly oxidized using 2,3-dichloro-5,6-dicyano-p-benzoquinone (DDQ) at first, and the filtered intermediate product subsequently continued to react with M5. In a way, it's essentially a ketoamine condensation reaction, yet the intermediates involved are neither isolated nor purified.

For some special class of monomers, such as M31 and M14, oxidants were not necessary, and the dehydration-oxidation tandem reaction went well under acidic and high-temperature conditions (HHTP-TABQ COF in Fig. 13) (Li et al., 2023a; Zhang et al., 2023a). The para quinone structure of M14, which could improve the reactivity of M14 and has a strong tendency to form conjugated structure, might be critical reasons for the indenpendance on oxidants.

3.2. Nucleophilic aromatic substitution reaction

Nucleophilic aromatic substitution (S_NAr) reaction has already been a very efficient synthesis method to prepare special engineering plastics such as polyetheretherketone (PEEK) and polysulfone (PSF). S_NAr reaction usually exhibits low reversibility because of the great difference in affinity between substrate and leaving group. Generally, the planarity of molecular skeleton will affect the successful synthesis of COF. The chemical bonds produced by S_NAr reaction are ether or amine bonds bearing high molecular flexibility, leading to the reduced alignment regularity of polymer chain during crystallization process, thus S_NAr reaction is rarely utilized to synthesize single-stranded COFs. Nevertheless, when it comes to the double-stranded ring linkers (such as dioxin and piperazine), the motion freedom of polymer chain would be greatly limited. Proper structural orientation, high reaction efficiency, together with intensive π-π interactions render S_NAr reaction to be another useful tool to build ladder-type COFs. On the contrary to the fully π-conjugated product of condensation reaction, S_NAr reaction generally results in non-conjugated COFs.

3.2.1. S_NAr reaction between hydroxyl and fluorine

The oxanthrene chromophore, which has two aromatic ether bonds and could be generated from aromatic catechol and aromatic-*ortho*-difluoro derivatives upon basic conditions, has been deeply investigated to synthesize PIMs (McKeown 2017; Low et al., 2018). Although only low porosity is observed for these amorphous linear polymers, these useful preparation experience provides a good platform for the synthesis of ladder-type COFs. Guan (Guan et al., 2019) firstly prepared this arylether-based COFs. In their study, M31 bearing C_3-symmetry was carried out to react with M23 and M25 with C_2-symmetry to give microporous COF (16.8 Å, JUC-505 in Fig. 14A) and mesoporous COF (28.4 Å, JUC-506 in Fig. 14A) via solvothermal synthesis method. Both COFs present hexagonal topology and eclipsed AA stacking structure on account of the strong π–π interactions between triphenylene subunits. Furthermore, both JUC-505 (1,584 $m^2 g^{-1}$) and JUC-506 (1,655 $m^2 g^{-1}$) possess ultrahigh BET surface areas, which are far more than their PIM partners.

At almost the same time, Zhang (Zhang et al., 2018) also reported the preparation of ladder-type COFs with the same structure. Except for M23, M24 bearing pyridine core was also attempted as a monomer to explore the application scope of S_NAr reactions, and the corresponding COF (COF-318 in Fig. 14A) were also successfully prepared. In addition to hydroxyl-based M31, thiophenol-based M32 was also exploited to prepare thianthrene-based COF (DUT-177 in Fig. 14A) as active material in lithium–sulfur battery. These S_NAr reactions were usually conducted using solvothermal synthesis method needed long reaction time (several days), and microwave-assisted synthesis was also confirmed to work for the S_NAr reaction while the preparation time could be greatly reduced to 30 min to 2 h (Ji et al., 2020; Kang et al., 2022). By the way, the presence of nitrile groups in the resulting COFs offers a great opportunity for the further functionalization of COFs via post-modification methods. For instance, JUC-505 was successfully transformed into carboxylic acid or carboxylate (Guo et al., 2022; Zhao et al., 2022a; Zhu et al., 2022; Su et al., 2023; Liu et al., 2024), amidoxime (Cheng et al., 2021; Li et al., 2022c), benzylamine (Guan et al., 2019), and thiocarbamoyl functionalized COFs (Zhao et al., 2023) (Fig. 14B). The characteristic of being easy to carry out post-synthetic modifications opens up a wide range of practical applications for these types of COFs.

Recently, a special monomer (M33) bearing a larger molecular size was also applied to construct ladder-type COF (HBC-TFPN in Fig. 14C) (Yu et al., 2022a). Although bearing a fused structure, it actually shows twisted skeleton with a double-bowled conformation. Indeed, the waviness of framework does not disrupt the interlayer π-π stacking, leading to the formation of crystalline COF. Except for the monomers with C_2-symmetry, M31 was also tried to combine with monomer

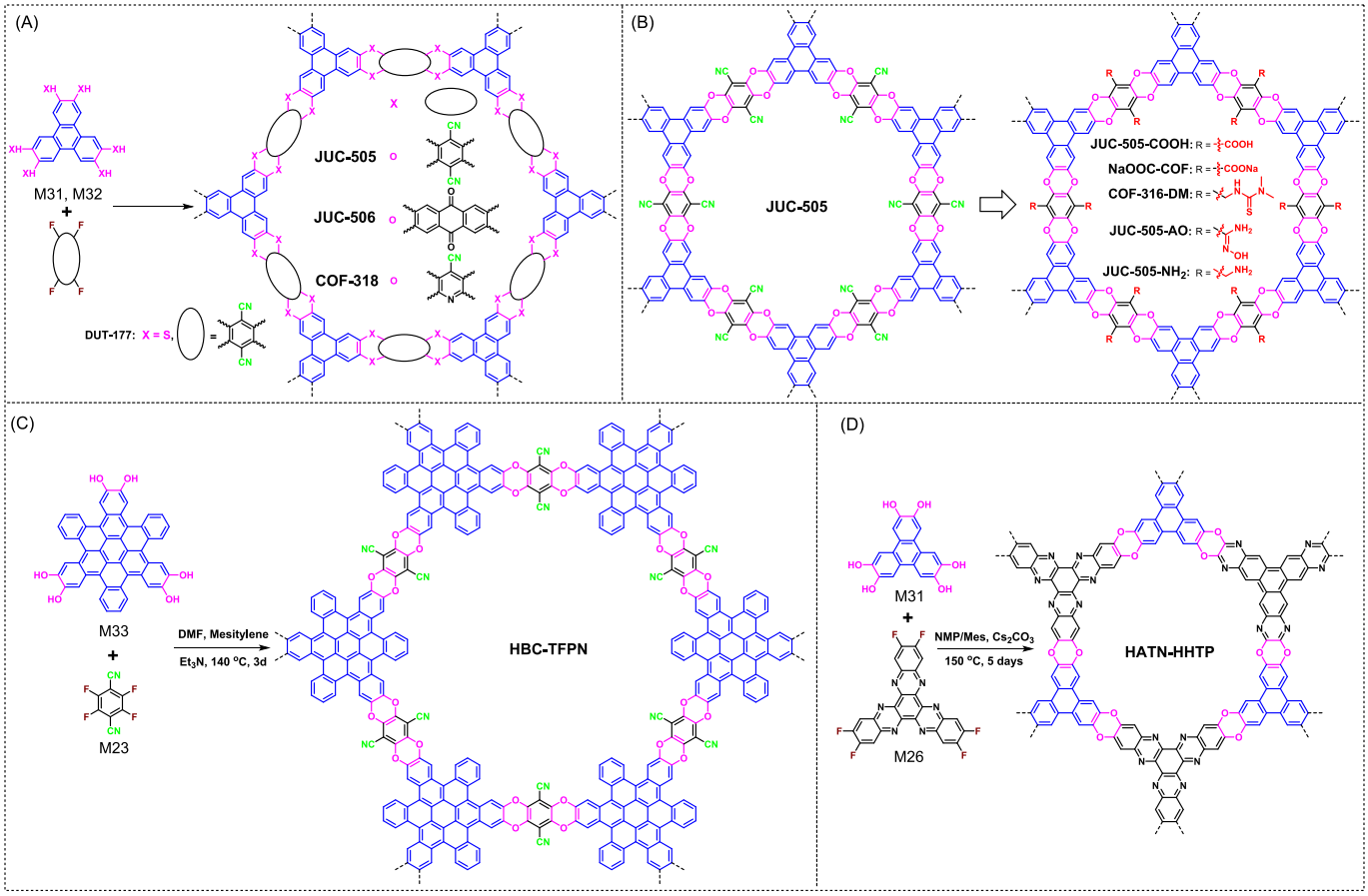

Fig. 14. (A) Synthesis of JUC-505, JUC-506, COF-318, and DUT-177 COFs through S_NAr reactions between C_3-symmetric catechols and C_2-symmetric aromatic-*ortho*-difluorines. (B) Synthesis of ladder-type COFs bearing different functional groups via post-modifications of JUC-505. (C) Synthesis of HBC-TFPN COF bearing twisted skeleton. (D) Synthesis of HATN–HHTP COF from C_3-symmetric M26 and M31.

bearing C_3-symmetry (such as M26), and the corresponding ladder-type COF (HATN–HHTP in Fig. 14D) was undoubtedly obtained (Li et al., 2022b). It should be emphasized that the strong electron-withdrawing nitriles and nitrogen atoms in polymerized monomers are believed to be essential for the S_NAr reactions. Otherwise, the departure of fluorine atoms will be difficult and the efficiency of unit reaction will be greatly reduced. In view of the above limitation, only limited monomers are selected to take S_NAr reactions. Developing more suitable monomers is an urgent task.

The above discussed $C_3 + C_2$ and $C_3 + C_3$ synthetic strategies produce COFs with only hexagonal pore in single layer. The introduction of monomers with C_4-symmetry would yield tetragonal pore. Given the many optical and electrical advantages of metallophthalocyanine as mentioned above, metallophthalocyanine building blocks are very good candidates. By virtue of the rich experiences in synthesizing boronate ester-based COFs, the selection of metallophthalocyanine monomer could be easily realized. Lu (Lu et al., 2021) achieved this goal through reacting catechol-based M34 with fluorine-based M23 under solvothermal conditions (Fig. 15A). The central atoms (*e.g.*, Cu, Ni, Co, and Zn) to modulate the structure–activity relationships of COFs could be easily regulated by selecting different polymerized monomers (Lei et al., 2021; Lu et al., 2021; Yang et al., 2021; Qiu et al., 2022). To expand the application scope of the reaction, the role of metallophthalocyanine was changed. M27 bearing sixteen fluorine atoms, of which eight fluorine atoms act as the leaving groups and another eight fluorine atoms ensure the electron-deficient feature of phthalocyanine core, was selected to react with different catechol derivatives (M28–M30) (Fig. 15B) (Wang et al., 2024b; Zhi et al., 2024). Confirming the reactivity of M27 in preparing ladder-type COFs, it was then polymerized with C_4-symmetric M34 or M35 to yield ladder-type COFs based entirely on metallophthalocyanines (Fig. 15C) (Yue et al., 2021a). Considering that the polymeric monomers are both metallophthalocyanine derivatives, it offers a great opportunity for preparing periodically bimetallic polymetallophthalocyanine COFs (Li et al., 2022a; Li et al., 2023b). Different metal atoms could interact within the framework between different metal centers as well as different layers, and it has shown that these interactions play crucial roles in enhancing the catalytic properties of resulting COFs (Yao et al., 2022).

The stable oxanthrene or thianthrene linkages provide these polyarylether-based COFs with superior chemical stability that could survive in various organic solvents (*e.g.*, m-cresol, DMF, EtOH, THF, NMP, DCM, and acetone) and even some extreme conditions including acids, bases, boiling water, oxidants, and reductants. As a matter of fact, the ultrahigh stability of oxanthrene or thianthrene motifs indicates the low reversibility of S_NAr reaction, and it is supposed that the strong rigidity of building blocks, the great directionality of linkages, the high conversion rate of S_NAr reaction, and the intensive π-π intermolecular interaction synergistically play indispensable roles in the formation of crystalline ladder-type COFs.

3.2.2. *S_NAr reaction between amine and fluorine*

In addition to hydroxyl group, aromatic fluorine could also occur in efficient S_NAr reaction with aromatic amine upon the catalysis of base, representing another alternative route to construct ladder-type COFs with piperazine motif serving as linkages. In comparison to pyrazine, piperazine-linked COFs supply not only abundant nitrogen atoms but also active hydrogen atoms to act as active sites, which plays an important role in practical applications. Different from hydroxyl groups

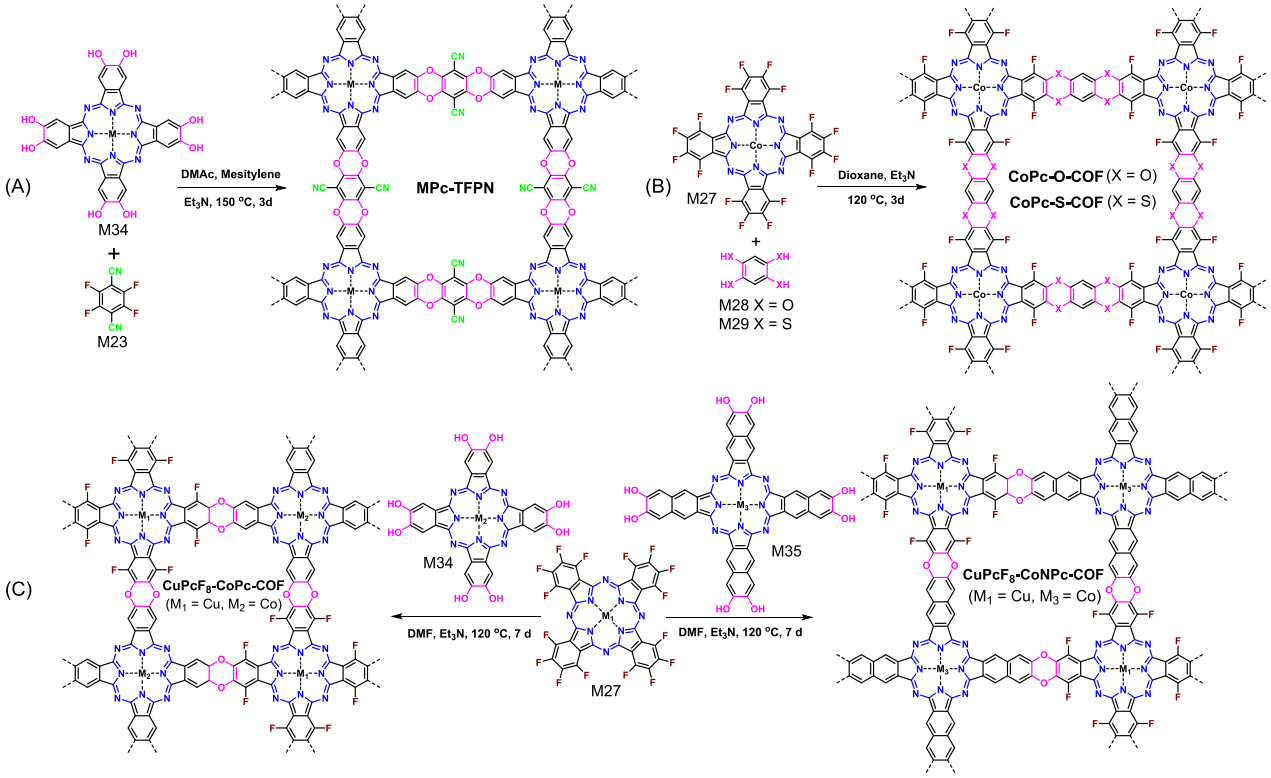

Fig. 15. Synthesis of (A) MPc-TFPN COF, (B) CoPC-O-COF as well as CoPc-S-COF, and (C) $CuPcF_8$-CoPc-COF as well as $CuPcF_8$-CoNPc-COF through S_NAr reactions between hydroxyl groups and fluorine atoms.

bearing various topological combinations, only $C_4 + C_2$ and $C_4 + C_4$ topological designs are successful in preparing ladder-type COFs when aromatic fluorine reacts with aromatic amine (Fig. 16). For aromatic electron-deficient fluorine, only M27 is reported up to date. In regard to aromatic amine, both linear (M12) (Zhi et al., 2022) and square (M11) (Yue et al., 2022) monomers are confirmed to work well. In practical applications, ladder-type COFs show great potential compared to their single-stranded COF partners. Zhi (Zhi et al., 2022) compared the photocatalytic performances of ladder-type CoPc-BTM-COF (structure sees Fig. 16) and its single-stranded counterpart CoPc-DAB-COF (structure sees Fig. 1). The ladder-type CoPc-BTM-COF reveal much greater conjugated length, leading to more intensive light absorption capacity in the range of 400–1000 nm and more facilitated photo-induced charge separation and transfer efficiency. Thus, CoPc-BTM-COF showed superior photocatalytic activity toward H_2O_2 photochemical synthesis (2096 μmol h^{-1} g^{-1} for CoPc-BTM-COF and 1851 μmol h^{-1} g^{-1} for single-stranded CoPc-DAB-COF). Notably, when the amines in M12 were partly replaced by thiophenol groups (that is M17), the reaction could still proceed successfully (CoPc-DNDS-COF in Fig. 16), indicating the high tolerance of the S_NAr reaction (Yang et al., 2023). All the piperazine-linked COFs showed well-defined porosity with high BET surface areas of 200–400 m^2 g^{-1} and were all observed to present AA eclipsed π-stacking mode owing to the intensive π-π interactions of metallophthalocyanine.

3.2.3. S_NAr reaction between amine and nitrile

As mentioned above, the nitrile group is highly reactive to convert into various functional groups. What's more, the nitrile group is also a

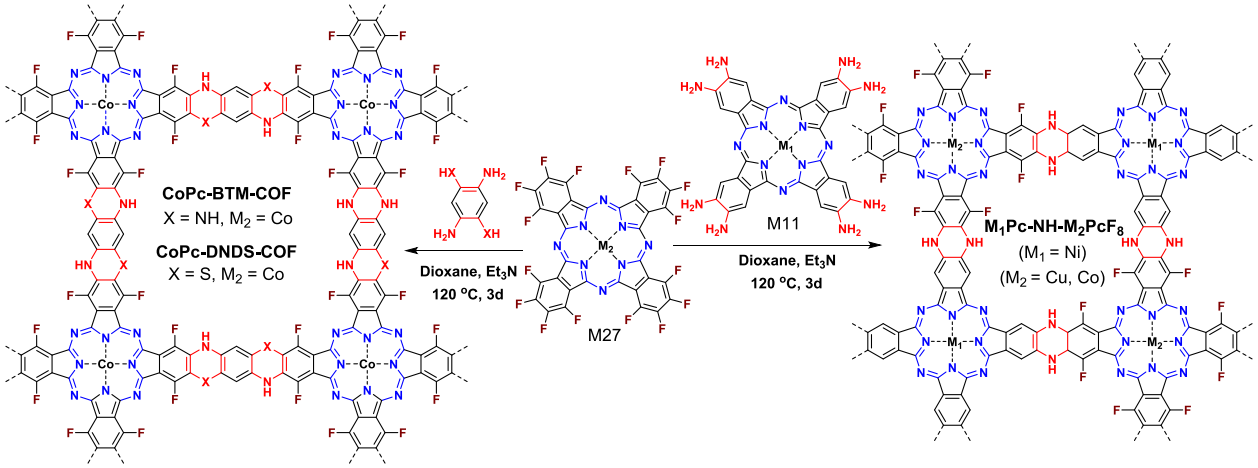

Fig. 16. Synthesis of CoPc-BTM-COF, CoPc-DNDS-COF, and M_1Pc-NH-M_2PcF8 COFs via S_NAr reactions between $MPcF_{16}$ and aromatic amines.

good leaving group, leading to efficient S_NAr reaction. In 2021, Kuehl (Kuehl et al., 2021) initially reported a series of piperazine-based ladder-type COFs through the S_NAr reaction of HAT-CN with different aromatic-*ortho*-diamines (COF3 and COF4 in Fig. 17). The electron-withdrawing HAT core ensures the successful leaving of nitriles. Given the nearly irreversible feature of the S_NAr reaction, the COFs were prepared through continuous optimizations that the optimal solvent, temperature, and reaction time were selected to NMP, 200 °C, and 24 h, respectively. COFs with different functional groups and pore sizes were modulated by choosing different aromatic amines (Wang et al., 2024a). The presence of bromine, carboxyl groups, and secondary amine provides favorable conditions for the post-synthetic modifications of COFs. For instance, the weakly basic N—H bond could react with trifluoroacetic anhydride or oxalyl chloride, resulting in trifluoroacetamide COF and cross-linking COF layers, respectively (Kuehl et al., 2021).

3.3. Coupling reaction

In order to get piperazine-based linkage, in addition to the above mentioned S_NAr reactions, coupling reaction could also achieve this goal. As a chemical bond with low bond energy, C-Br bonds play active roles in various coupling reactions. In fact, various coupling reactions have been widely applied for the synthesis of different POPs such as HCPs, CMPs, and PAFs (Evans et al., 2022). Although most of the polymerized products are amorphous polymers, however, it is entirely possible to get COFs and even ladder-type COFs through delicate monomer selection and proper reaction condition manipulations. Recently, Zhou (Zhou et al., 2021) reported a piperazine-based ladder-type COFs (PTDCOF in Fig. 18) via Buchwald–Hartwig cross-coupling (BHCC) reaction with 2,3,6,7,10,11-hexabromotriphenylene (HBTP) and M5 as two monomers. Both bearing triphenylene as molecular core, the planar and triangularly orientated configuration of M5 and HBTP monomers provides proper topological constraint to the formation of crystalline structure, and the COF structure was undoubtedly confirmed by various methods. Furthermore, because the pores in PTDCOF are tightly occupied by guest molecules (*e.g.*, methanol), an ambiguous AA eclipsed together with AB staggered stacking mode and a relatively low BET surface area (32.6 $m^2\ g^{-1}$) were concluded. More effort is in demand to better manipulate this type of reaction.

4. Conclusions and outlooks

COFs truly shine as the superstars within the family of POPs. In comparison to the single-stranded COFs, ladder-type COFs are connected by rings, thus they are provided with the merits of rigid backbone, great π-conjugation length, outstanding chemical/thermal stability, and superior conductivity. Considering the multiple-stranded linking mode, the fabrication of ladder-type COFs is a very attractive and challenging job, which needs high requirements in the rigidity and topological structure of monomers, the efficiency and reversibility of chemical reaction, the number and orientation of functional groups, and the precise control of operating conditions. Up to now, there are generally three types of reactions that successfully achieve the construction of ladder-type COFs, including condensation reaction, S_NAr reaction, and coupling reaction. Condensation reaction usually results in fully conjugated COFs while S_NAr reaction and coupling reaction generally contribute to non-conjugated skeletons. Various functional groups, including aromatic ketone, amine, nitrile, fluorine and hydroxyl groups, play pivotal roles in constructing these COFs. The resulting ring linkages, including pyrazine, piperazine, metallophthalocyanine, oxanthrene or thianthrene, are mostly π-conjugated and rich in various heteroatoms (*e.g.*, N, O, and S), providing valuable active sites for practical applications. Metallophthalocyanine is the most successful monomer and polymerized product, which not only has a rigid backbone and large conjugated length that contribute to strong π-π intermolecular interactions, but also it is easily derivable and suitable for various types of reactions. Moreover, the feasible regulation of the central metal atoms provides more convenience for modulating the electronic property.

The past few years have witnessed the rapid developments of ladder-type COFs. However, compared to the fully developed single-stranded connecting COFs, ladder-type COFs are still in its infancy. In regard to the design and synthesis of ladder-type COFs, the following research areas may be worthy of the continuous attention from scientists. (1) Expanding the variety of reactions and topologies. More than twenty reactions can be used to construct single-stranded COFs bearing diverse topologies, but only limited reactions can be applied for preparing hexagonal or tetragonal ladder-type COFs. It's in great demand to develop more efficient reactions and expand more topologies. (2) Fabrication of 3D ladder-type COFs. In comparison to 2D COFs, 3D COFs are endowed with ultrahigh BET surface areas that result in more active sites. However, compared to a wide variety of 3D single-stranded COFs, no 3D ladder-type COFs was reported. Careful selection of monomers and reactions as well as precise manipulation of reaction conditions are of significant importance. Triptycene- or spirocycle-based monomers might be good candidates (Ahmad et al., 2020). (3) Deep understanding of reaction mechanism and precise control of reaction conditions. For the same monomers, different operating conditions lead to more amorphous polymers than crystalline COFs. To gain ladder-type COFs with regular structure, high crystallinity, and stable property, it is necessary to explore the detailed mechanisms of polymerization and crystallization processes in depth to find the chief influencing factor on COFs and to better manipulate the reaction conditions. (4) Developing large-scale preparation techniques for ladder-type COFs. Laboratory preparation techniques are usually on the milligram scale, which have the characteristics of high equipment requirements, complicated operation procedures, and high cost. Developing commercially viable

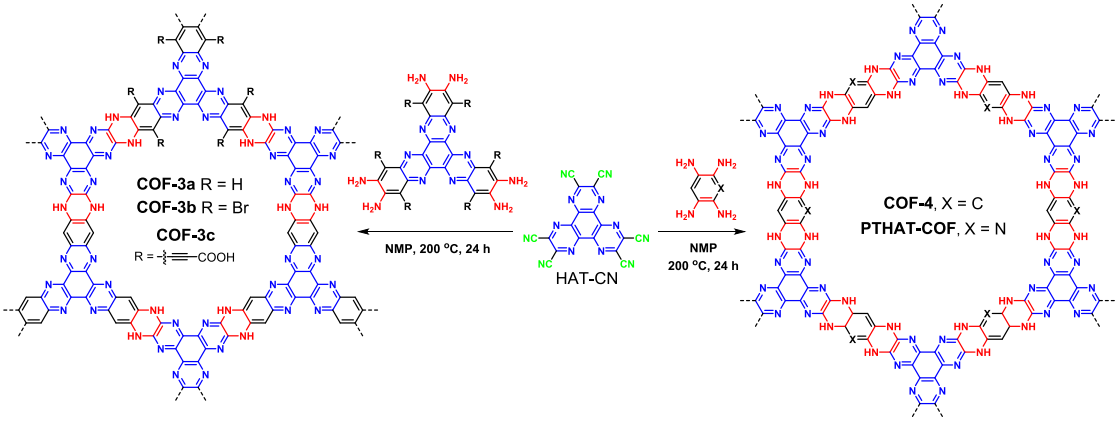

Fig. 17. Synthesis of piperazine-based COFs via nucleophilic substitution reaction between aromatic nitrile and aromatic amines.

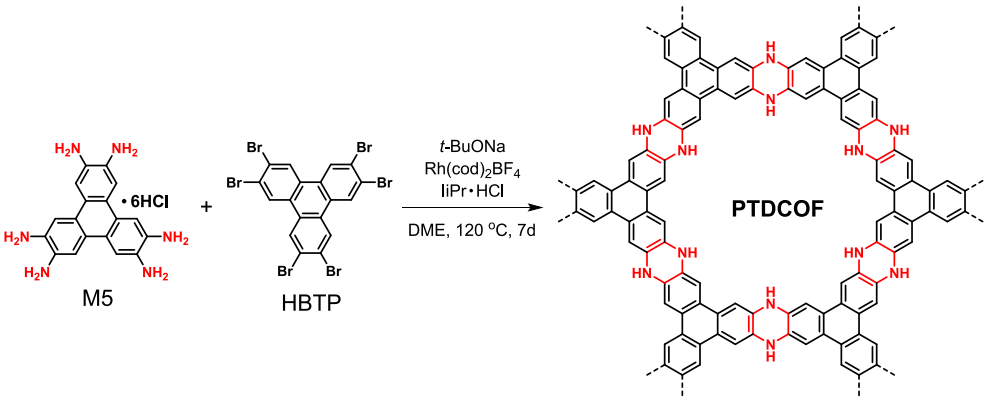

Fig. 18. Synthesis of PTDCOF via Buchwald–Hartwig cross-coupling reaction.

material preparation technique for large-scale production are also worthy of deep exploration. High-gravity intensified synthesis offers an alternative solution (Zhao et al., 2022b). In addition, the preparation of ladder-type COF in film form is also a meaningful and attractive topic since the products of reported COFs are mainly presented in powder form.

Funding statement

This research was funded by the Scientific Research Foundation for Advanced Talents, Chongqing Technology and Business University (No. 1956054, No. 1956055, and No. 2056014).

CRediT authorship contribution statement

Hongfei Sun: Writing – original draft. **Xianying Wu:** Writing – review & editing. **Bin Yao:** Writing – review & editing. **Guowang Li:** Methodology. **Ning Qi:** Supervision. **Lei Shi:** Writing – review & editing.

Declaration of competing interest

The authors declare that they have no known competing financial interests or personal relationships that could have appeared to influence the work reported in this paper.

Acknowledgement

This paper is dedicated to Professor Xinhua Wan on the occasion of his 60th birthday.

References

Ahmad, I., Mahmood, J., Baek, J.-B., 2020. Recent progress in porous fused aromatic networks and their applications. Small Sci. 1, 2000007.
Arora, N., Flores, C., Senarathna, M.C., et al., 2024. Design, synthesis, and applications of mesoporous covalent organic frameworks. CCS Chem. 6, 57–68.
Bai, Y., Liu, Y., Liu, M., et al., 2022. Near-equilibrium growth of chemically stable covalent organic framework/graphene oxide hybrid materials for the hydrogen evolution reaction. Angew. Chem. Int. Ed. 61, e202113067.
Che, S., Fang, L., 2020. Porous ladder polymer networks. Chem. 6, 2558–2590.
Chen, H., Suo, X., Yang, Z., et al., 2022. Graphitic aza-fused π-conjugated networks: Construction, engineering, and task-specific applications. Adv. Mater. 34, 2107947.
Chen, J., Zou, K., Ding, P., et al., 2019. Conjugated cobalt polyphthalocyanine as the elastic and reprocessable catalyst for flexible Li-CO_2 batteries. Adv. Mater. 31, 1805484.
Cheng, G., Zhang, A., Zhao, Z., et al., 2021. Extremely stable amidoxime functionalized covalent organic frameworks for uranium extraction from seawater with high efficiency and selectivity. Sci. Bull. 66, 1994–2001.
Côté, A.P., Benin, A.I., Ockwig, N.W., et al., 2005. Porous, crystalline, covalent organic frameworks. Science 310, 1166–1170.
Das, S., Heasman, P., Ben, T., et al., 2017. Porous organic materials: strategic design and structure-function correlation. Chem. Rev. 117, 1515–1563.
Duong, P.H.H., Kuehl, V.A., Mastorovich, B., et al., 2019. Carboxyl-functionalized covalent organic framework as a two-dimensional nanofiller for mixed-matrix ultrafiltration membranes. J. Membr. Sci. 574, 338–348.
Evans, A.M., Parent, L.R., Flanders, N.C., et al., 2018. Seeded growth of single-crystal two-dimensional covalent organic frameworks. Science 361, 52–57.
Evans, A.M., Strauss, M.J., Corcos, A.R., et al., 2022. Two-dimensional polymers and polymerizations. Chem. Rev. 122, 442–564.
Gao, Y., Tan, Z., Yang, R., et al., 2022. Integrating polyarylether-COFs with TiO_2 nanofibers for enhanced visible-light-driven CO_2 reduction in artificial photosynthesis. Appl. Surf. Sci. 605, 154605.
Geng, K., Arumugam, V., Xu, H., et al., 2020a. Covalent organic frameworks: Polymer chemistry and functional design. Prog. Polym. Sci. 108, 101288.
Geng, K., He, T., Liu, R., et al., 2020b. Covalent organic frameworks: design, synthesis, and functions. Chem. Rev. 120, 8814–8933.
Guan, X., Li, H., Ma, Y., et al., 2019. Chemically stable polyarylether-based covalent organic frameworks. Nat. Chem. 11, 587–594.
Guan, X., Fang, Q., Yan, Y., et al., 2022. Functional regulation and stability engineering of three-dimensional covalent organic frameworks. Acc. Chem. Res. 55, 1912–1927.
Guo, J., Xu, Y., Jin, S., et al., 2013. Conjugated organic framework with three-dimensionally ordered stable structure and delocalized pi clouds. Nat. Commun. 4, 2736.
Guo, H., Xu, X., Li, J., et al., 2022. Chemically tailored microporous nanocomposite membranes with multi-channels for intensified solvent permeation. J. Membr. Sci. 660, 120877.
Han, J., Feng, J., Kang, J., et al., 2024. Fast growth of single-crystal covalent organic frameworks for laboratory x-ray diffraction. Science 383, 1014–1019.
Han, X., Yuan, C., Hou, B., et al., 2020. Chiral covalent organic frameworks: design, synthesis and property. Chem. Soc. Rev. 49, 6248–6272.
Haug, W.K., Moscarello, E.M., Wolfson, E.R., et al., 2020. The luminescent and photophysical properties of covalent organic frameworks. Chem. Soc. Rev. 49, 839–864.
He, J., Hong, H., Feng, Q., et al., 2022. Conjugated cobalt polyphthalocyanine with defective π-π extended structure for enhanced rechargeable li-oxygen batteries. Chem. Eng. J. 444, 136544.
Huang, N., Lee, K.H., Yue, Y., et al., 2020a. A stable and conductive metallophthalocyanine framework for electrocatalytic carbon dioxide reduction in water. Angew. Chem. Int. Ed. 59, 16587–16593.
Huang, X., Sun, C., Feng, X., 2020b. Crystallinity and stability of covalent organic frameworks. Sci. China Chem. 63, 1367–1390.
Jhulki, S., Kim, J., Hwang, I.-C., et al., 2020. Solution-processable, crystalline π-conjugated two-dimensional polymers with high charge carrier mobility. Chem 6, 2035–2045.
Ji, W., Guo, Y.S., Xie, H.M., et al., 2020. Rapid microwave synthesis of dioxin-linked covalent organic framework for efficient micro-extraction of perfluorinated alkyl substances from water. J. Hazard Mater. 397, 122793.
Jiang, M., Han, L., Peng, P., et al., 2022. Quasi-phthalocyanine conjugated covalent organic frameworks with nitrogen-coordinated transition metal centers for high-efficiency electrocatalytic ammonia synthesis. Nano Lett. 22, 372–379.
Jin, E., Asada, M., Xu, Q., et al., 2017. Two-dimensional sp^2 carbon–conjugated covalent organic frameworks. Science 357, 673–676.
Kang, D.W., Kim, J.H., Lim, J.H., et al., 2022. Promoted type I and II ROS generation by a covalent organic framework through sonosensitization and PMS activation. ACS Catal. 12, 9621–9628.
Kim, S.J., Mahmood, J., Kim, C., et al., 2018. Defect-free encapsulation of Fe^0 in 2D fused organic networks as a durable oxygen reduction electrocatalyst. J. Am. Chem. Soc. 140, 1737–1742.
Kitao, T., Zhang, X., Uemura, T., 2022. Nanoconfined synthesis of conjugated ladder polymers. Polym. Chem. 13, 5003–5018.
Kuehl, V.A., Yin, J., Duong, P.H.H., et al., 2018. A highly ordered nanoporous, two-dimensional covalent organic framework with modifiable pores, and its application in water purification and ion sieving. J. Am. Chem. Soc. 140, 18200–18207.
Kuehl, V.A., Duong, P.H.H., Sadrieva, D., et al., 2021. Synthesis, postsynthetic modifications, and applications of the first quinoxaline-based covalent organic framework. ACS Appl. Mater. Interfaces 13, 37494–37499.

Lee, J.-S.-M., Cooper, A.I., 2020. Advances in conjugated microporous polymers. Chem. Rev. 120, 2171–2214.
Lei, Z., Lucas, F.W.S., Canales Moya, E., et al., 2021. Highly stable dioxin-linked metallophthalocyanine covalent organic frameworks. Chinese Chem. Lett. 32, 3799–3802.
Li, X., 2021. sp^2 carbon-conjugated covalent organic frameworks: synthesis, properties, and applications. Mater. Chem. Front. 5, 2931–2949.
Li, N., Jiang, K., Rodríguez-Hernández, F., et al., 2022a. Polyarylether-based 2D covalent-organic frameworks with in-plane D-A structures and tunable energy levels for energy storage. Adv. Sci. 9, 2104898.
Li, N., Gao, H., Liu, Z., et al., 2023b. Metalphthalocyanine frameworks grown on TiO_2 nanotubes for synergistically and efficiently electrocatalyzing urea production from CO_2 and nitrate. Sci. China Chem. 66, 1417–1424.
Li, S., Liu, Y., Dai, L., et al., 2022b. A stable covalent organic framework cathode enables ultra-long cycle life for alkali and multivalent metal rechargeable batteries. Energy Storage Mater. 48, 439–446.
Li, X., Wang, H., Chen, H., et al., 2020. Dynamic covalent synthesis of cystalline porous graphitic frameworks. Chem 6, 933–944.
Li, M., Zeng, F., Li, S., et al., 2023a. Unlocking high-performance organic cathodes: tailoring active group densities in covalent frameworks for aqueous zinc ion batteries. Energy Mater. Devices 1, 9370007.
Li, Z., Zhu, R., Zhang, P., et al., 2022c. Functionalized polyarylether-based COFs for rapid and selective extraction of uranium from aqueous solution. Chem. Eng. J. 434, 134623.
Liang, R.R., Jiang, S.Y., et al., 2020. Two-dimensional covalent organic frameworks with hierarchical porosity. Chem. Soc. Rev. 49, 3920–3951.
Liang, R.-R., Zhao, X., 2018. Heteropore covalent organic frameworks: a new class of porous organic polymers with well-ordered hierarchical porosities. Org. Chem. Front. 5, 3341–3356.
Liu, M., Guo, L., Jin, S., et al., 2019a. Covalent triazine frameworks: synthesis and applications. J. Mater. Chem. a. 7, 5153–5172.
Liu, X., Huang, D., Lai, C., et al., 2019b. Recent advances in covalent organic frameworks (COFs) as a smart sensing material. Chem. Soc. Rev. 48, 5266–5302.
Liu, Y., Ma, Y., Zhao, Y., et al., 2016. Weaving of organic threads into a crystalline covalent organic framework. Science 351, 365–369.
Liu, Y., Wang, M., Hui, Y., et al., 2024. Polyarylether-based COFs coordinated by Tb^{3+} for the fluorescent detection of anthrax-biomarker dipicolinic acid. J. Mater. Chem. B 12, 466–474.
Liu, X., Zhang, A., Ma, R., et al., 2022. Experimental and theoretical insights into copper phthalocyanine-based covalent organic frameworks for highly efficient radioactive iodine capture. Chinese Chem. Lett. 33, 3549–3555.
Low, Z.-X., Budd, P.M., McKeown, N.B., et al., 2018. Gas permeation properties, physical aging, and its mitigation in high free volume glassy polymers. Chem. Rev. 118, 5871–5911.
Lu, M., Zhang, M., Liu, C.-G., et al., 2021. Stable dioxin-linked metallophthalocyanine covalent organic frameworks (COFs) as photo-coupled electrocatalysts for CO_2 reduction. Angew. Chem. Int. Ed. 60, 4864–4871.
Luo, S., Zeng, Z., Wang, H., et al., 2021. Recent progress in conjugated microporous polymers for clean energy: Synthesis, modification, computer simulations, and applications. Prog. Polym. Sci. 115, 101374.
Ma, Y., Liu, X., Guan, X., et al., 2019. One-pot cascade syntheses of microporous and mesoporous pyrazine-linked covalent organic frameworks as Lewis-acid catalysts. Dalton Trans. 48, 7352–7357.
Ma, T., Zhou, Y., Diercks, C.S., et al., 2023. Catenated covalent organic frameworks constructed from polyhedra. Nat. Synth. 2, 286–295.
Mahmood, J., Anjum, M.A.R., Baek, J.B., 2019. Fused aromatic network structures as a platform for efficient electrocatalysis. Adv. Mater. 31, 1805062.
Mahmood, J., Ahmad, I., Jung, M., et al., 2020. Two-dimensional amine and hydroxy functionalized fused aromatic covalent organic framework. Commun. Chem. 3, 31.
McKeown, N.B., 2017. The synthesis of polymers of intrinsic microporosity (PIMs). Sci. China Chem. 60, 1023–1032.
Meng, Z., Aykanat, A., Mirica, K.A., 2019a. Proton conduction in 2D aza-fused covalent organic frameworks. Chem. Mater. 31, 819–825.
Meng, Z., Stolz, R.M., Mirica, K.A., 2019b. Two-dimensional chemiresistive covalent organic framework with high intrinsic conductivity. J. Am. Chem. Soc. 141, 11929–11937.
Niu, K., Zhang, Y., Chen, J., et al., 2022. 2D Conductive covalent organic frameworks with abundant carbonyl groups for electrochemical sensing. ACS Sens. 7, 3551–3559.
Noh, H.-J., Im, Y.-K., Yu, S.-Y., et al., 2020. Vertical two-dimensional layered fused aromatic ladder structure. Nat. Commun. 11, 2021.
Pan, Y., Wang, M., Li, M., et al., 2022. In-situ construction of N-doped carbon nanosnakes encapsulated FeCoSe nanoparticles as efficient bifunctional electrocatalyst for overall water splitting. J. Energy Chem. 68, 699–708.
Parvatkar, P.T., Kandambeth, S., Shaikh, A.C., et al., 2023. A tailored COF for visible-light photosynthesis of 2,3-dihydrobenzofurans. J. Am. Chem. Soc. 145, 5074–5082.
Pei, C., Ben, T., Qiu, S., 2015. Great prospects for PAF-1 and its derivatives. Mater. Horiz. 2, 11–21.
Peng, P., Shi, L., Huo, F., et al., 2019. In situ charge exfoliated soluble covalent organic framework directly used for Zn-air flow battery. ACS Nano 13, 878–884.
Phan, P.T., Ta, Q.T.H., Nguyen, P.K.T., 2023. Designed synthesis of three-dimensional covalent organic frameworks: a mini review. Polymers 15, 887.
Pourghasem, S., Moeinpour, F., Mohseni-Shahri, F.S., 2023. Cu(II)/polyimide linked COF: An effective mesoporous catalyst for solvent-free 1,5-benzodiazepine synthesis. Arabian J. Chem. 16, 104694.
Qi, N., Yao, B., Sun, H., et al., 2023. Anthraquinone-based porous organic polymers: From synthesis to applications in electrochemical energy conversion and storage. Arabian J. Chem. 16, 105263.
Qin, L., Ma, C., Zhang, J., et al., 2024. Structural motifs in covalent organic frameworks for photocatalysis. Adv. Funct. Mater. 35, 2401562.
Qiu, X.-F., Huang, J.-R., Yu, C., et al., 2022. A stable and conductive covalent organic framework with isolated active sites for highly selective electroreduction of carbon dioxide to acetate. Angew. Chem. Int. Ed. 61, e202206470.
Segura, J.L., Mancheño, M.J., Zamora, F., 2016. Covalent organic frameworks based on Schiff-base chemistry: synthesis, properties and potential applications. Chem. Soc. Rev. 45, 5635–5671.
Seob, S.K., Fritz, P.W., Abbott, D.F., et al., 2023. Mixed-metal ionothermal synthesis of metallophthalocyanine covalent organic frameworks for CO_2 capture and conversion. Angew. Chem. Int. Ed. 62, e202309775.
Shehab, M.K., Weeraratne, K.S., Huang, T., et al., 2021. Exceptional sodium-ion storage by an aza-covalent organic framework for high energy and power density sodium-ion batteries. ACS Appl. Mater. Interfaces 13, 15083–15091.
Shi, R., Liu, L., Lu, Y., et al., 2020. Nitrogen-rich covalent organic frameworks with multiple carbonyls for high-performance sodium batteries. Nat. Commun. 11, 178.
Shin, S.-H., Noh, H.-J., Kim, Y.-H., et al., 2019. Forming layered conjugated porous BBL structures. Polym. Chem. 10, 4185–4193.
Su, L.-H., Qian, H.-L., Yang, C., et al., 2023. Surface imprinted-covalent organic frameworks for efficient solid-phase extraction of fluoroquinolones in food samples. J. Hazard Mater. 459, 132031.
Sun, T., Xie, J., Guo, W., et al., 2020. Covalent–organic frameworks: advanced organic electrode materials for rechargeable batteries. Adv. Energy Mater. 10, 1904199.
Tahir, N., Krishnaraj, C., Leus, K., et al., 2019. Development of covalent triazine frameworks as heterogeneous catalytic supports. Polymers 11, 1326.
Tian, Y., Zhu, G., 2020. Porous aromatic frameworks (PAFs). Chem. Rev. 120, 8934–8986.
Tran, Q.N., Lee, H.J., Tran, N., 2023. Covalent organic frameworks: From structures to applications. Polymers 15, 1279.
Walczak, R., Kurpil, B., Savateev, A., et al., 2018. Template- and metal-free synthesis of nitrogen-rich nanoporous "noble" carbon materials by direct pyrolysis of a preorganized hexaazatriphenylene precursor. Angew. Chem. Int. Ed. 57, 10765–10770.
Waller, P.J., Gandara, F., Yaghi, O.M., 2015. Chemistry of covalent organic frameworks. Acc. Chem. Res. 48, 3053–3063.
Wang, M., Ballabio, M., Wang, M., et al., 2019. Unveiling electronic properties in metal-phthalocyanine-based pyrazine-linked conjugated two-dimensional covalent organic frameworks. J. Am. Chem. Soc. 141, 16810–16816.
Wang, M., Fu, S., Petkov, P., et al., 2023. Exceptionally high charge mobility in phthalocyanine-based poly(benzimidazobenzophenanthroline)-ladder-type two-dimensional conjugated polymers. Nat. Mater. 22, 880–887.
Wang, W., Kale, V.S., Cao, Z., et al., 2020a. Phenanthroline covalent organic framework electrodes for high-performance zinc-ion supercapattery. ACS Energy Lett. 5, 2256–2264.
Wang, W., Kale, V.S., Cao, Z., et al., 2021. Molecular engineering of covalent organic framework cathodes for enhanced zinc-ion batteries. Adv. Mater. 33, 2103617.
Wang, C., Li, R., Zhu, Y., et al., 2024a. A pyrazine-pyridinamine covalent organic framework as a low potential anode for highly durable aqueous calcium-ion batteries. Adv. Energy Mater. 14, 2302495.
Wang, R., Lyu, H., Poon Ho, G.S.H., et al., 2024b. Highly conductive covalent-organic framework films. Small 20, 2306634.
Wang, Z., Zhang, S., Chen, Y., et al., 2020b. Covalent organic frameworks for separation applications. Chem. Soc. Rev. 49, 708–735.
Wang, X., Zhou, Z., Lin, X., et al., 2022. Nanostructured hexaazatrinaphthalene based polymers for advanced energy conversion and storage. Chem. Eng. J. 427, 130995.
Weng, J., Xi, Q., Zeng, X., et al., 2022. Recent progress of hexaazatriphenylene-based electrode materials for rechargeable batteries. Catal. Today 400–401, 102–114.
Wu, J.S., Cheng, S.W., Cheng, Y.J., et al., 2015. Donor-acceptor conjugated polymers based on multifused ladder-type arenes for organic solar cells. Chem. Soc. Rev. 44, 1113–1154.
Xiao, L., Wang, Z., Guan, J., 2023. Optimization strategies of covalent organic frameworks and their derivatives for electrocatalytic applications. Adv. Funct. Mater. 34, 2310195.
Xie, M., Li, C., Ren, S., et al., 2022. Ultrafine Sb nanoparticles in situ confined in covalent organic frameworks for high-performance sodium-ion battery anodes. J. Mater. Chem. A 10, 15089–15100.
Xu, S., Luo, Y., Tan, B., 2013. Recent development of hypercrosslinked microporous organic polymers. Macromol. Rapid Commun. 34, 471–484.
Yang, X., Gong, L., Wang, K., et al., 2022a. Ionothermal synthesis of fully conjugated covalent organic frameworks for high-capacity and ultrastable potassium-ion batteries. Adv. Mater., 2207245
Yang, C., Jiang, K., Zheng, Q., et al., 2021. Chemically stable polyarylether-based metallophthalocyanine frameworks with high carrier mobilities for capacitive energy storage. J. Am. Chem. Soc. 143, 17701–17707.
Yang, X., Jin, Y., Yu, B., et al., 2022b. Two-dimensional conjugated N-rich covalent organic frameworks for superior sodium storage. Sci. China Chem. 65, 1291–1298.
Yang, X., Li, X., Liu, M., et al., 2023. Modulating electrochemical CO_2 reduction performance via sulfur-containing linkages engineering in metallophthalocyanine based covalent organic frameworks. ACS Mater. Lett. 5, 1611–1618.
Yang, X., Li, X., Liu, M., et al., 2024. Quantitative construction of boronic-ester linkages in covalent organic frameworks for the carbon dioxide reduction. Angew. Chem. Int. Ed. 63, e202317785.

Yang, C., Yang, Z.-D., Dong, H., et al., 2019. Theory-driven design and targeting synthesis of a highly-conjugated basal-plane 2D covalent oganic framework for metal-free electrocatalytic OER. ACS Energy Lett. 4, 2251–2258.
Yang, S., Yu, Y., Dou, M., et al., 2020. Edge-functionalized polyphthalocyanine networks with high oxygen reduction reaction activity. J. Am. Chem. Soc. 142, 17524–17530.
Yao, B., He, Y., Wang, S., et al., 2022. Recent advances in porphyrin-based systems for electrochemical oxygen evolution reaction. Int. J. Mol. Sci. 23, 6036.
Yao, B., Li, G., Wu, X., et al., 2024. Polyimide covalent organic frameworks bearing star-shaped electron-deficient polycyclic aromatic hydrocarbon building blocks: molecular innovations for energy conversion and storage. Chem. Commun. 60, 793–803.
Yu, J., Chen, X., Wang, H.-G., et al., 2022b. Conjugated ladder-type polymers with multielectron reactions as high-capacity organic anode materials for lithium-ion batteries. Sci. China. Mater. 65, 2354–2362.
Yu, H.-Y., Wang, J.-S., Xie, F.-Y., et al., 2022a. A stack-guiding unit constructed 2D COF with improved charge carrier transport and versatile photocatalytic functions. Chem. Eng. J. 445, 136713.
Yue, Y., Cai, P., Xu, K., et al., 2021a. Stable bimetallic polyphthalocyanine covalent organic frameworks as superior electrocatalysts. J. Am. Chem. Soc. 143, 18052–18060.
Yue, Y., Cai, P., Xu, X., et al., 2021b. Conductive metallophthalocyanine framework films with high carrier mobility as efficient chemiresistors. Angew. Chem. Int. Ed. 60, 10806–10813.
Yue, Y., Li, H., Chen, H., et al., 2022. Piperazine-linked covalent organic frameworks with high electrical conductivity. J. Am. Chem. Soc. 144, 2873–2878.
Yusran, Y., Guan, X., Li, H., et al., 2020. Postsynthetic functionalization of covalent organic frameworks. Natl. Sci. Rev. 7, 170–190.
Zhang, W., Chen, L., Dai, S., et al., 2022b. Reconstructed covalent organic frameworks. Nature 604, 72–79.
Zhang, Y., Jin, S., 2018. Recent advancements in the synthesis of covalent triazine frameworks for energy and environmental applications. Polymers 11, 31.
Zhang, Y., Huang, Z., Ruan, B., et al., 2020b. Design and synthesis of polyimide covalent organic frameworks. Macromol. Rapid Commun. 41, 2000402.
Zhang, M.D., Si, D.H., Yi, J.D., et al., 2020a. Conductive phthalocyanine-based covalent organic framework for highly efficient electroreduction of carbon dioxide. Small 16, 2005254.
Zhang, M., Tong, Y., Sun, Z., et al., 2023a. Two-dimensional covalent organic framework with synergistic active centers for efficient electrochemical sodium storage. Chem. Mater. 35, 4873–4881.
Zhang, Z., Wang, W., Wang, X., et al., 2022c. Ladder-type π-conjugated metallophthalocyanine covalent organic frameworks with boosted oxygen reduction reaction activity and durability for zinc-air batteries. Chem. Eng. J. 435, 133872.
Zhang, B., Wei, M., Mao, H., et al., 2018. Crystalline dioxin-linked covalent organic frameworks from irreversible reactions. J. Am. Chem. Soc. 140, 12715–12719.
Zhang, J.-L., Yao, L.-Y., Yang, Y., et al., 2022a. Conductive covalent organic frameworks with conductivity- and pre-reduction-enhanced electrochemiluminescence for ultrasensitive biosensor construction. Anal. Chem. 94, 3685–3692.
Zhang, Y., Zhang, X., Jiao, L., et al., 2023c. Conductive covalent organic frameworks of polymetallophthalocyanines as a tunable platform for electrocatalysis. J. Am. Chem. Soc. 145, 24230–24239.
Zhang, S., Zhu, Y.-L., Ren, S., et al., 2023b. Covalent organic framework with multiple redox active sites for high-performance aqueous calcium ion batteries. J. Am. Chem. Soc. 145, 17309–17320.
Zhao, F., Bai, Y., Zhou, X., et al., 2023. An aryl-ether-linked covalent organic framework modified with thioamide groups for selective extraction of palladium from strong acid solutions. Chem. Eur. J. 29, e202302445.
Zhao, G., Xu, L., Jiang, J., et al., 2022a. COFs-based electrolyte accelerates the Na^+ diffusion and restrains dendrite growth in quasi-solid-state organic batteries. Nano Energy 92, 106756.
Zhao, Y., Yu, X., Wen, X., et al., 2022b. HiGee strategy towards large-scale synthesis of soluble covalent organic frameworks. AIChE J. 69, e17864.
Zhi, Q., Liu, W., Jiang, R., et al., 2022. Piperazine-linked metalphthalocyanine frameworks for highly efficient visible-light-driven H_2O_2 photosynthesis. J. Am. Chem. Soc. 144, 21328–21336.
Zhi, Q., Jiang, R., Yang, X., et al., 2024. Dithiine-linked metalphthalocyanine framework with undulated layers for highly efficient and stable H_2O_2 electroproduction. Nat. Commun. 15, 678.
Zhi, Y., Wang, Z., Zhang, H.L., et al., 2020. Recent progress in metal-free covalent organic frameworks as heterogeneous catalysts. Small 16, 2001070.
Zhong, H., Wang, M., Ghorbani-Asl, M., et al., 2021. Boosting the electrocatalytic conversion of nitrogen to ammonia on metal-phthalocyanine-based two-dimensional conjugated covalent organic frameworks. J. Am. Chem. Soc. 143, 19992–20000.
Zhou, R., Huang, Y., Li, Z., et al., 2021. Piperazine-based two-dimensional covalent organic framework for high performance anodic lithium storage. Energy Storage Mater. 40, 124–138.
Zhu, C., Kalin, A.J., Fang, L., 2019. Covalent and noncovalent approaches to rigid coplanar π-conjugated molecules and macromolecules. Acc. Chem. Res. 52, 1089–1100.
Zhu, J., Yuan, S., Wang, J., et al., 2020. Microporous organic polymer-based membranes for ultrafast molecular separations. Prog. Polym. Sci. 110, 101308.
Zhu, R., Zhang, P., Zhang, X., et al., 2022. Fabrication of synergistic sites on an oxygen-rich covalent organic framework for efficient removal of Cd(II) and Pb(II) from water. J. Hazard Mater. 424, 127301.
Zou, G., Tian, Z., Kale, V.S., et al., 2023. A symmetric aqueous magnesium ion supercapattery based on covalent organic frameworks. Adv. Energy Mater. 13, 2203193.